THE ASTROPHYSICAL JOURNAL, SUPPLEMENT SERIES, 41:301–326, 1979 October


# SCALE COVARIANCE AND G-VARYING COSMOLOGY. IV. THE LOG N–LOG S RELATION

V. M. CANUTO*
NASA Goddard Institute for Space Studies, Goddard Space Flight Center
AND
J. R. OWEN
Department of Physics, City College of the City of New York
*Received 1978 December 8; accepted 1979 March 19*

## ABSTRACT

The traditional radio counts $N(S)$ and radio source models are studied within the framework of the scale-covariant cosmology developed to investigate whether the relative strength of the gravitational and electromagnetic constants is a function of cosmological epoch. It is found that a gravitational constant $G$ varying as $t^{-1}$, where $t$ is the epoch in atomic units, is consistent with all the data analyzed. For a wide class of models, the present cosmology allows a finer discrimination of the deceleration parameter than does standard theory. The results, when combined with those of previous papers, namely those from radio and optical flux and angular diameter data analysis, favor an open universe.

*Subject headings:* cosmology — gravitation — radio sources: galaxies

## I. INTRODUCTION

It is the purpose of this paper to study the normalized, differential form of the log $N$–log $S$ relation for radio sources within the framework of the scale-covariant cosmology developed and tested in previous papers. The formulation of the theory is described by Canuto *et al.* (1977, hereafter Paper I); the formulation of thermodynamics and the 3 K background radiation is described by Canuto and Hsieh (1979, hereafter Paper II). The magnitude-redshift test, the radio angular diameter–redshift test, and the optical number-magnitude test are described in Canuto, Hsieh, and Owen (1979, hereafter Paper III). In Paper III an improvement over non–scale-covariant cosmology was obtained in fitting the data for a choice of parameters consistent with the present physical understanding of evolution. In the same paper a good fit to the large $N(m)$ versus $m$ slope for QSOs was also achieved. These tentative successes impel one to seek substantiation of the theory with further tests. The analysis of number counts, i.e., the number of sources having an observed flux greater than $S$, is an interesting case in point since 15 years of model fitting under the assumptions of standard (non–scale-covariant) cosmology have yielded a discrepancy with the data which is rather insensitive to the parameters of that cosmology and which has been lumped into a free "evolutionary function" as described below. We shall demonstrate in this paper that the full covariant model needs to ascribe less of the fundamental form of the data to an "evolutionary function," which besides is not free at all. Indeed the standard theory does not depend sensibly on the deceleration parameter $\bar{q}_0$ while the scale-covariant theory can. This increases our confidence in the possibility of determining the curvature of the universe when all tests are in. For a similar sensitivity of the results to the value of $\bar{q}_0$, see the tests described in Paper III.

Petrosian (1969), using the integrated $N(S)$ count, found that the 3C data were consistent with the Lemaître model with a uniform distribution of sources, but he had to use a $(1 + z)^{1.5}$ evolutionary law to reconcile the 4C and 5C data with this model. Furthermore, the differential form of the test would have been superior statistically (Jauncey 1967, 1975). The calculations for a $\bar{q}_0 = \sigma_0 = 1$ model required substantial evolution, namely, $(1 + z)^{4 \pm 1}$.

Von Hoerner (1973) obtained a satisfactory fit by using a "flat" radio luminosity function (RLF), a density function $(1 + z)^3 F(z)$, with $F(z)$ made to order from the data, and a relaxed redshift cutoff. A "critical" luminosity function would require in addition a luminosity slope evolution to make the RLF flatter in the past (making it no longer really critical, of course). A "parabolic" RLF would require in addition a luminosity range evolution. His results were presented for a modified $\bar{q}_0 = \sigma_0 = 1$ model (taking advantage of the insensitivity to $\bar{q}_0$) and for a spectral index $\alpha$ equal to $-1$.

Wall, Pearson, and Longair (1977), using the Einstein–de Sitter model, found their best fit for an evolutionary function $E(L, z)$ which depends on four parameters. They did not have the same success when they applied the model to a sample at higher frequencies containing a wider gamut of spectral indices, presumably because the

* Also with the Department of Physics, CCNY.

RLF of the steep sources which show up at high frequencies is different from that of those which show up at low frequencies.

Recently Robertson (1978) has presented a free-form iterative calculation of the luminosity distribution required to produce the observed differential log $N$–log $S$ curve assuming an Einstein–de Sitter model, $\alpha = -0.9$, and no evolution of luminosities inferior to a critical luminosity. His results approximate the $(1 + z)^5$ power law (used in previous studies with a cutoff) up to $z \sim 3$, after which they level off and possibly decrease with $z$.

In all of the previous calculations, ad hoc evolutionary effects were assumed to fit the data. Their very existence rules out all simpler versions of the steady-state theory which have no room for evolution. Using the scale-covariant theory, it turns out that part of the ad hoc evolution is accounted for by the new geometry, i.e., by the scale used, so that the large exponents like $(1 + z)^{4-5}$ are here reduced. It also turns out that, in contrast to the standard case, most chosen scales when combined with the data put constraints on the acceptable deceleration parameter $\bar{q}_0$.

In § II we present a derivation of the log $N$–log $S$ relation for the near region. This has the advantage of being easily interpretable, and it can be made to produce the characteristically steep slope of $-2.2$ at high $S$ in the quasar counts (Véron 1966). This turns out to be possible if we use a model with a maximum in the effective luminosity distance $\zeta_L$. The definition and behavior of $\zeta_L$ are explained in § III, and both new and old reasons for the observed luminosity-redshift distribution are offered.

In § IV we present the derivation of the expression for the differential count and the conditions under which it is computed. In § V we present several analytic cases.

Section VI is dedicated to the discussion of the RLF. We have performed computations (*a*) by calculating the RLF within the context of the present theory and (*b*) by "assuming" a RLF to allow comparison with previous results. The 177 sources used in this work are drawn mostly from the 4C survey and have known redshifts, spectral indices, and radio diameters. We also reran the program with a set compiled by Soltan (1978*a*, *b*) with criteria of completeness. In order to make full use of the available information, we used the spectral index characteristic of each source instead of the common convenient practice of one average index for all sources.

In § VII we discuss the results, and in § VIII we present the final discussion.

## II. THE NUMBER COUNT

The scale-covariant theory as described in Papers I, II, and III posits that the gravitational (or "Einstein") and electromagnetic (or "atomic") line elements, $d\bar{s}$ and $ds$, which form the basis of their respective dynamical theories, are related by a time-dependent scale function $\beta(t)$,

$$d\bar{s} = \beta(t)ds\,; \qquad \beta(t_0) \equiv 1\,. \tag{2.1}$$

Equation (2.1) implies that gravitational and electromagnetic interactions did not always have the relative strengths observed today. All quantities calculated within the gravitational theory are indicated by a bar, except the redshifts which we denote by $\varkappa$. Quantities ultimately derivable from quantum electrodynamic theory or observed through atomic processes are unbarred, including the redshift $z$ (see Paper III, eqs. [3.1] and [3.2]). The scale function $\beta$ in (2.1) is a function of atomic time. Current research has concentrated on the consequences of assuming a general form

$$\beta(t) = (t_0/t)^{\epsilon} \quad (\epsilon = \pm 1, \pm \tfrac{1}{2})\,. \tag{2.2}$$

Two gauges, i.e., two values of $\epsilon$, were suggested by Dirac (1938, 1974): $\epsilon = \pm 1$; the other two were suggested by the present authors (Papers II and III). $\bar{R}(\bar{t})$ appearing in Einstein's theory is related to the scale factor $R(t)$ as it is observed through atomic processes by the scale factor $\beta(t)$ (II, eqs. [2.1]–[2.5]).

The full solution of the gravitational equations written in atomic units as well as the behavior of $\beta(t)$, $R(t)$ versus $t$; and $z$ can be found in Paper III, Tables 1–4.

To find $dN(t_e)$, the total number of radio sources which emitted their light after time $t_e$, we must first find the number of galaxies enclosed between coordinates $r_e$ and $r_e + dr_e$ at time $t_e$. If we assume a Robertson-Walker metric and if $n(t)$ is the number of galaxies per unit proper volume, we have

$$dN(t_e) = n(t)4\pi r_e^2 R^2(t)R(t)dr_e(1 - kr_e^2)^{-1/2}\,. \tag{2.3}$$

If the radio source density depends only on expansion, i.e., if there is no net creation or destruction of sources, then

$$n(t)R^3(t) = n_0 R_0{}^3\,. \tag{2.4}$$

Using the relation

$$dr_e(1 - kr_e^2)^{-1/2} = cdt_e/R(t_e)\,, \tag{2.5}$$

we find that the total number of sources that emitted their light after $t_e$ is given by

$$N(>t_e) = 4\pi c n_0 R_0^3 \int_{t_e}^{t_0} r_e^2(t) \frac{dt}{R(t)} . \tag{2.6}$$

In the present section, we shall concentrate on the high flux regime. Expanding $R(t)$ in the usual form

$$R(t) = R_0[1 - H_0(t_0 - t) + \cdots] \tag{2.7}$$

so that

$$r_e(t) = (c/R_0)[t_0 - t + \tfrac{1}{2}H_0(t_0 - t)^2] , \tag{2.8}$$

we have

$$N(>t_e) = 4\pi n_0 c^3 (t_0 - t_e)^3 [1 + \tfrac{3}{2}H_0(t - t_e)] . \tag{2.9}$$

If the source obeys a synchrotron-type power law

$$P(\nu_e)d\nu_e \sim \nu_e^{\alpha} d\nu_e , \tag{2.10}$$

with the redshift law (III, eq. [3.1])

$$\frac{\nu_e}{\nu_0} = 1 + z = \frac{R_0}{R(t_e)} , \tag{2.11}$$

we obtain the radio bolometric correction

$$P(\nu_e)d\nu_e \sim \nu_0^{\alpha} R(t_e)^{-(1+\alpha)} d\nu_0 . \tag{2.12}$$

Within the scale-covariant theory the universal gravitational "constant" $G$ is written in general as (see Papers I and II)

$$G = G_0 \beta^{-\pi_g} \equiv G_0 \beta^{-g} . \tag{2.13}$$

As far as evolution is concerned, we shall generalize the expression used in standard cosmology, namely,

$$L(t) = L(t_0)(1 + z)^E , \tag{2.14}$$

to

$$L(t) = L(t_0)\beta^e(t) \equiv L_0 \beta^e(t) . \tag{2.15}$$

(For the inclusion of density evolution, see comment after eq. [4.4] and Paper III, § XIII.) Then equation (III, 7.4) becomes

$$L_0/4\pi S = R_0^2 r_e^2 (R_0/R)^{1-\alpha} \beta^{g-2-e} . \tag{2.16}$$

Substituting the expansion (III, eq. [5.12]) for $\beta$

$$\beta(t) = 1 + \frac{\epsilon}{t_0}(t_0 - t) + \cdots \tag{2.17}$$

and (2.7) and (2.8), we obtain

$$t_0 - t = \frac{1}{c}\left(\frac{L_0}{4\pi S}\right)^{1/2}\left[1 - \frac{(2 - \alpha)}{2}\frac{H_0}{c}\left(\frac{L_0}{4\pi S}\right)^{1/2}(1 - C_1)\right] , \tag{2.18}$$

where

$$C_1 \equiv \frac{\epsilon(2 + e - g)}{(2 - \alpha)H_0 t_0} . \tag{2.19}$$

Substitution of (2.18) into (2.9) yields

$$N(>S) = \frac{4\pi n_0}{3}\left(\frac{L_0}{4\pi S}\right)^{3/2}\left[1 - \tfrac{3}{2}(1 - \alpha)\frac{H_0}{c}\left(\frac{L_0}{4\pi S}\right)^{1/2}(1 - C_2)\right] \tag{2.20}$$

with

$$C_2 \equiv \frac{\epsilon(2 + e - g)}{(1 - \alpha)H_0 t_0} = \frac{2 - \alpha}{1 - \alpha} C_1 .$$

In the optical case (obtained by setting $\alpha = -1$), equation (2.20) reduces to equation (III, 12.23) as expected. In

the case of standard cosmology, $\epsilon = 0$ and $g = 0$, equation (2.20) reduces to equation (14.735) of Weinberg (1972) or to equation (13.36) of von Hoerner.

From (2.20) we can easily evaluate the slope of the $N$-$S$ curve,

$$\text{slope} = \frac{S}{N}\frac{dN}{dS} = -\frac{3}{2}\left[1 - \frac{(1-\alpha)}{2}\frac{H_0}{c}\left(\frac{L_0}{4\pi S}\right)^{1/2}(1 - C_2)\right].$$

Using the well-known expansion

$$H_0(t_0 - t) \simeq z[1 - (1 + \tfrac{1}{2}q_0)z]$$

in (2.18), we finally obtain

$$\frac{H_0}{c}\left(\frac{L_0}{4\pi S}\right)^{1/2} = z\left\{1 + z\left[\left(\frac{2-\alpha}{2}\right)(1 - C_1) - (1 + \tfrac{1}{2}q_0)\right]\right\},$$

so that to first order in $z$

$$\text{slope} = \frac{S}{N}\frac{dN}{dS} = -\frac{3}{2}\left[1 - \frac{(1-\alpha)}{2}(1 - C_2)z\right]. \tag{2.21}$$

The first term in (2.21) reproduces the well-known Euclidian result, $S^{-3/2}$, whereas the term in parentheses represents the correction due to cosmology. Contrary to standard cosmology, the second term in brackets can be made positive if $C_2 > 1$, thus increasing the slope from $-1.5$ to perhaps $-2.2$, the observed value for quasars. This can indeed be achieved if

$$(1 - \alpha)H_0 t_0 < \epsilon(2 + e - g). \tag{2.22}$$

The values of $e$ which produce a slope steeper than $-1.5$ assuming $\epsilon g = -1$ and $\alpha = -0.75$ are given in column (A) of Table 1. By multiplying $e$ by the numbers in column (D) one obtains the equivalent $E$ in standard cosmology for an assumed evolutionary function $(1 + z)^E$ (see [2.14] and § VII). In a real sample, the sources have a wide range of redshifts of course. When $z$ becomes very small, the required $|e|$ for a slope of $-2.2$ is very large except for $\epsilon > 0$. We might not have to take such a stringent requirement as a slope of $-2.2$ (which comes from sources with large as well as small redshifts). We must realize that, once evolution is assumed, there is no reason to wish it to be small or large as long as it is consistent with the other tests and the model of physical evolution.

## III. THE LUMINOSITY DISTANCE

Using (III, 7.5),

$$r_e = \frac{c}{\bar{R}_0\bar{H}_0}\frac{F(\varkappa, \bar{q}_0)}{(1 + \varkappa)}, \tag{3.1}$$

let us rewrite the exact expression (2.16) as

$$L_0 = 4\pi(c/\bar{H}_0)^2 S\zeta_L^2(\beta), \tag{3.2}$$

TABLE 1

EVOLUTIONARY PARAMETER $e$

| $\bar{q}_0$ | $\epsilon$ | $H_0t_0$ | A | B | C | D | E |
|---|---|---|---|---|---|---|---|
| 0..... | $-1$ | 1 | $-2.75$ | $-6.75$ | $-6.85$ | $-1$ | $-5$ |
| | $-\frac{1}{2}$ | 1 | $-3.50$ | $-9.50$ | $-9.96$ | $-\frac{1}{2}$ | $-10$ |
| | $+\frac{1}{2}$ | 1 | $-0.50$ | $+1.50$ | $+3.50$ | $+\frac{1}{2}$ | $+10$ |
| | $+0.92$ | 1 | $-1.18$ | $-1.01$ | $+0.80$ | $+0.92$ | $+5.435$ |
| | $+1$ | 1 | $-1.25$ | $-1.25$ | ... | $+1$ | $+5$ |
| $\frac{1}{2}$..... | $-1$ | $\frac{1}{3}$ | $-1.58$ | $-1.58$ | $-1.75$ | $-3$ | $-1.67$ |
| | $-\frac{1}{2}$ | $\frac{1}{2}$ | $-1.75$ | $-1.75$ | $-2.75$ | $-1$ | $-5$ |
| | $+\frac{1}{2}$ | $\frac{5}{6}$ | $-1.08$ | $-1.08$ | $+1.96$ | $+0.6$ | $+8.333$ |
| | $+0.92$ | 0.97 | $-1.24$ | $-1.24$ | $+0.66$ | $+0.945$ | $+5.290$ |
| | $+1$ | 1 | $-1.25$ | $-1.25$ | ... | $+1$ | $+5$ |
| 1..... | $-1$ | 0.1416 | $-1.25$ | $-1.24$ | ... | $-7.06$ | $-0.708$ |
| | $-\frac{1}{2}$ | 0.3562 | $-1.25$ | $-1.24$ | ... | $-1.40$ | $-3.56$ |
| | $+\frac{1}{2}$ | 0.7854 | $-1.25$ | $-1.25$ | $+1.075$ | $+0.637$ | $+7.854$ |
| | $+0.92$ | 0.9651 | $-1.25$ | $-1.25$ | $+0.612$ | $+0.953$ | $+5.248$ |
| | $+1$ | 1 | $-1.25$ | $-1.25$ | ... | $+1$ | $+5$ |

NOTE.—Columns (A)–(E) are as follows: (A) Values of $e$ that give $d\log N/d\log S < -1.5$ (eq. [2.23], $\alpha = -0.75$). (B) Values of $e$ that give $z_* = \infty$ (eq. [3.7], $p = -1, -2$, $\alpha = -0.75$). (C) Values of $e$ that give $z_* = 2$ (eqs. [3.4], [3.7], and [3.8], $\alpha = -0.75$). (D) The ratio $E/e$ in general as given by eq. (7.1). (E) Values of $e$ that give $E = 5$ (eq. [7.1]).

where we have introduced the "luminosity distance"

$$\zeta_L(\beta) = F(\varkappa, \bar{q}_0)(1 + \varkappa)^{-(1+\alpha)/2}\beta^x; \qquad 2x \equiv g - 1 - \alpha - e, \tag{3.3}$$

which merely tries to incorporate into one expression evolutionary, geometrical, and bolometric factors contributing to the relationship between $L$ and $S$.

Note that as given in equation (3.3), $\zeta_L$ is a function of $\varkappa$ (the redshift in gravitational units, not that observed in atomic units) and of $\beta$ which is usually given as a function of atomic time $t$. In standard cosmology, $\beta = 1$, $\varkappa = z$, and so (3.2) and (3.3) together reduce to the standard equations describing both the $S$-$z$ diagram for any $\alpha$ and the $m$-$z$ diagram if we take $\alpha = -1$. We note that for suitable choice of $x$, it is possible for the luminosity distance $\zeta_L$ to have a maximum, $\zeta_L{}^*$, at redshift $z_*$. In standard cosmology, it is also possible to have a maximum in the luminosity distance but evolution must be very strong to make it occur at observable redshifts if $\bar{q}_0$ is not very large. The interest in a luminosity distance which is a slowly increasing function of $\varkappa$ or which has even a maximum is that such a behavior seems indicated by the radio $S$-$z$ diagram and by the integrated $N(S)$ counts. The data cannot yet establish its existence in the available redshift range $z \leq 3.5$, so if a maximum exists, it must be at $z > 2$ at least or else it would be more evident.

The presence of an observable maximum in standard cosmology would imply a closed universe and/or very strong evolution. However, because of the presence of the scale function $\beta(t)$, and the facts that $\varkappa \neq z$ and that our evolutionary function cannot in general be parametrized as $(1 + z)^E$, it is to be expected that the value of $z_*$ will be different in scale-covariant theory than in standard theory for the same $\bar{q}_0$. For some choices of $\epsilon$ and only moderate or null evolution it is possible to have $\zeta_L{}^*$ occur at observable or nearly observable $z_*$ in an open universe. Thus for some scale choices, the $S$-$z$ diagram corresponding to an open universe in our cosmology will look like the $S$-$z$ diagram within a closed universe of standard cosmology. Similarly as the results for $m$ versus $z$ and $\theta_m$ versus $z$ of Paper III indicate, it is possible within our theory and an open universe to obtain results that in standard theory can only be obtained with a closed universe. For the $\theta_i$ versus $z$ test, as explained in Paper III, the results of our theory can be simulated by standard theory by either a higher or a lower $\bar{q}_0$ depending on the gauge $\epsilon$ and $\bar{q}_0$ chosen.

This explains the inconsistency of the results of the various cosmological tests (which require the angular distance to increase more swiftly than the luminosity distance with $z$) as interpreted by standard theory but which require a unique $\bar{q}_0$ in the scale-covariant theory. These remarks become particularly important if it turns out that the measured deuterium abundance implies an open universe also in the new theory; this is a problem now under investigation.

*A priori* we should not expect the optical data to behave the same way. However, the steep slope of the $N$ versus $m$ diagram can in fact imply a maximum in the bolometric distance as discussed in Paper III, §§ XII and XIII. Also the $m$ versus $z$ diagram combining the QSO and galactic data shows signs of a maximum, a circumstance which is variously interpreted as evidence for high $\bar{q}_0$, galactic evolution, misinterpretation of the redshift, or the unsuitability of QSOs for the test. The similarity of the behavior of the optical and radio data may be due to their physical connection which fortuitously is leading to similar evolutionary rates (perhaps density evolution would be easier to understand than luminosity evolution in this context), or it may be that geometrical considerations and/or strong selection effects based on geometry are the dominant factors in both radio and optical flux distributions and a corrected (e.g., scale covariant) interpretation of spacetime is in order.

Let us now study the cases $\bar{q}_0 = 0, \frac{1}{2}$ which can be treated analytically and the case $\bar{q}_0 = 1$ in the limit of small $z$. From equation (III, 3.3) we now have the exact results

$$\begin{aligned} 1 + z = \beta(1 + \varkappa) &= (1 + \varkappa)^{1/(1-\epsilon)} \qquad (\bar{q}_0 = 0,\ \bar{H}_0\bar{t}_0 = 1); \\ 1 + z = \beta(1 + \varkappa) &= (1 + \varkappa)^{(2+\epsilon)/(2-2\epsilon)} \quad (\bar{q}_0 = \tfrac{1}{2},\ \bar{H}_0\bar{t}_0 = \tfrac{2}{3}). \end{aligned} \tag{3.4}$$

For $\bar{q}_0 = 1$, since $R(\bar{t}) \sim \bar{t}^{H_0\bar{t}_0}$ for $\varkappa \ll 1$, it follows that

$$1 + z = \beta(1 + \varkappa) \sim (1 + \varkappa)^{1 - \epsilon/H_0\bar{t}_0/(\epsilon - 1)} \quad (\bar{q}_0 = 1,\ \bar{H}_0\bar{t}_0 = \pi/2 - 1). \tag{3.5}$$

Using now (3.3) we can write

$$\zeta_L(\varkappa) = F(\varkappa, \bar{q}_0)(1 + \varkappa)^p, \tag{3.6a}$$

where (III, 7.6a)

$$F(\varkappa, \bar{q}_0) = \varkappa + \frac{\varkappa^2(1 - \bar{q}_0)}{1 + \bar{q}_0\varkappa + (1 + 2\bar{q}_0\varkappa)^{1/2}} \tag{3.6b}$$

and

$$2p = \frac{\epsilon(e + \alpha + 1 - g)}{(\epsilon - 1)\bar{H}_0\bar{t}_0} - (1 + \alpha). \tag{3.7}$$

Using equation (3.6b), it is easy to find that the maximum of $\zeta_L$ occurs at

$$1 + z^* = \left(\frac{p}{2+p}\right)^{1/2} \quad (p \leq -2, \bar{q}_0 = 0),$$

$$1 + z_* = \left(\frac{p+\frac{1}{2}}{p+1}\right)^2 \quad (p \leq -1, \bar{q}_0 = \tfrac{1}{2}),$$

$$1 + z_* = \frac{p}{p+1} \quad (p \leq -1, \bar{q}_0 = 1). \tag{3.8}$$

The values of $e$ corresponding to $p = -2$ and $-1$ (yielding $z_* = z = \infty$) are plotted as a function of $\epsilon$ for $\alpha = -0.75$ in Figure 1*a* ($\bar{q}_0 = 0$) and for $\alpha = -0\,25$, $-0.5$, and $-0.75$ in Figure 1*b* ($\bar{q}_0 = \frac{1}{2}$). The values of $e$ for the average spectral index $\alpha = -0.75$ are presented in column (B) of Table 1. The region above the curve for $\epsilon < 0$ and below the curve for $\epsilon > 0$ is denoted Region I and corresponds to values of $p$ for which $\zeta_L$ has no maximum at real, positive $z$. The remaining area is denoted Region II and corresponds to the condition for a maximum. We note that when $\bar{q}_0 = \frac{1}{2}$, $\alpha = -\frac{1}{2}$ and when $\bar{q}_0 = 1$, $\alpha = -0.7519$, $z \sim 0$, the division corresponds to the coordinate axes. In general as $|\alpha|$ becomes smaller or $\bar{q}_0$ becomes greater, Region II becomes larger. As we penetrate deeper into Region II in all cases (taking $e$ farther from the boundary for the same $\epsilon$), $p$ becomes more negative, and $z_*$ (as well as $z_*$) becomes smaller.

Although $e = 0$ is not expected in the present cosmology, for the sake of understanding, the $p$ values corresponding to no evolution are given in Table 2 as a function of $\alpha$ and $\epsilon$. It is seen that except for unusually flat spectral indices and approximately for $\bar{q}_0 = 1$ in the local region, there is very little hope in the standard cosmology of finding $p$ in Region II, a region so useful for understanding the $S$-$z$ and $m$-$z$ diagrams and the high slopes in the counts $N(m)$ and $N(\text{high } S)$. When $g\epsilon = -1$ and $e = 0$, we have

$$p = p(\epsilon = 0) + \frac{1}{2}\frac{\epsilon(\alpha + 2)}{(\epsilon - 1)\bar{H}_0 \bar{t}_0}. \tag{3.9}$$

If $0 > \epsilon > 1$, the $\epsilon \neq 0$ contribution is positive and we are less likely to find a maximum for $\zeta_L$ at real positive $z$ (Region II). If $0 < \epsilon < 1$, the contribution from the $\epsilon$ term is negative and we are more likely to be in Region II even without postulating any evolution.

Since we require that the maximum, if it occurs, occur at $2 < z_* < \infty$, we have calculated the combinations of $(\epsilon, e, \alpha)$ which would yield $z_* = 2$ and present $e(z^* = 2)$ in column (C) of Table 1. When $\bar{q}_0 = 1$, we include only

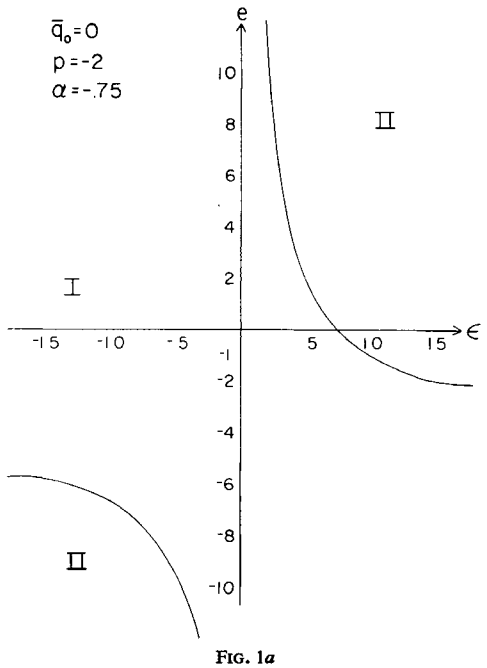


FIG. 1*a*

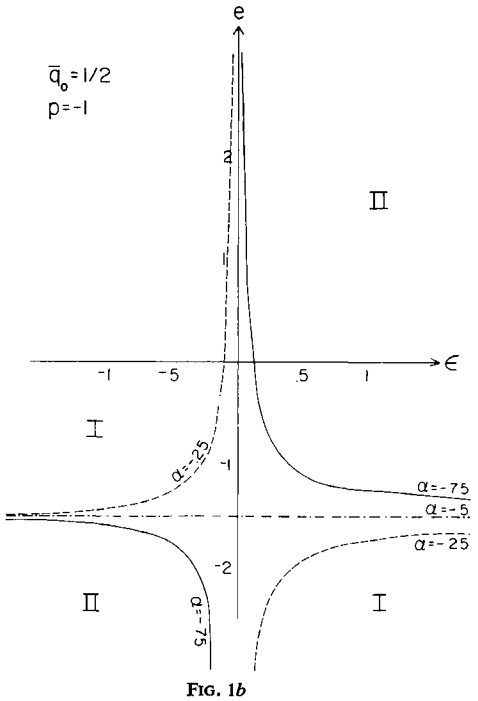


FIG. 1*b*

FIG. 1.—Evolutionary parameter $e$ versus scale parameter $\epsilon$ satisfying eq. (3.7) for (*a*) $p = -2$ ($\bar{q}_0 = 0$), and (*b*) $p = -1$ ($\bar{q}_0 = \frac{1}{2}$), giving $z_* = \infty$.

TABLE 2

EXPONENT $p$ AS A FUNCTION OF $\alpha$ AND $\epsilon$ WHEN THERE IS NO EVOLUTION ($e = 0$) AS GIVEN BY EQUATIONS (3.7) ($e = 0$, $g_*\epsilon = -1$)

| $\bar{q}_0$ | $\alpha/\epsilon$ | $-1.00$ | $-0.50$ | 0.00 | 0.50 | 0.92 |
|---|---|---|---|---|---|---|
| 0..... | $-0.25$ | $-0.438$ | $-0.584$ | $-0.875$ | $-1.750$ | $-10.94$ |
| | $-0.50$ | $-0.375$ | $-0.500$ | $-0.750$ | $-1.500$ | $-9.38$ |
| | $-0.75$ | $-0.312$ | $-0.416$ | $-0.625$ | $-1.250$ | $-7.81$ |
| | $-1.00$ | $-0.250$ | $-0.333$ | $-0.500$ | $-1.000$ | $-6.25$ |
| 0.50..... | $-0.25$ | $-0.562$ | $-0.688$ | $-1.125$ | $-2.438$ | $-16.22$ |
| | $-0.50$ | $-0.500$ | $-0.625$ | $-1.000$ | $-2.125$ | $-13.94$ |
| | $-0.75$ | $-0.438$ | $-0.562$ | $-0.875$ | $-1.812$ | $-11.66$ |
| | $-1.00$ | $-0.375$ | $-0.500$ | $-0.750$ | $-1.500$ | $-9.38$ |
| 1.00..... | $-0.25$ | $-0.484$ | $-0.740$ | $-1.251$ | $-2.786$ | $-18.88$ |
| | $-0.50$ | $-0.469$ | $-0.683$ | $-1.126$ | $-2.441$ | $-16.24$ |
| | $-0.75$ | $-0.454$ | $-0.636$ | $-1.001$ | $-2.096$ | $-13.59$ |
| | $-1.00$ | $-0.438$ | $-0.584$ | $-0.876$ | $-1.752$ | $-10.95$ |

NOTE.—When $p \leq -1$ or $-2$ ($\bar{q}_0 = 0$), we can expect that data if available to show a maximum in the luminosity distance which is not due to evolution but merely to the scale geometry and (constant) source spectral properties.

$\epsilon > 0$ because the $\varkappa_*$ corresponding to $\epsilon < 0$ is too great for the approximation. Examination of columns (C) and (B) reveals that except for $\epsilon > 0$, for a given ($\epsilon$, $\alpha$) the $e$ (and $p$) do not change significantly between $z_* = 2$ and $z_* = \infty$ and $e$ is therefore fairly well determined if we accept the hypothesis that the solution is in Region II. We point out that, contrary to the case in standard cosmology, within the scale-covariant cosmology $z_*$ may occur at observable values (i.e., $z_* \lesssim 4$) even in an open universe. Requiring $z_* > 4$ then serves to restrict $e$ to a small range between columns (B) and (C).

We draw the reader's attention to the fact that for $\bar{q}_0 = \frac{1}{2}$, the condition that $z_* = \infty$ (that is, the boundary between Regions I and II, eq. [3.7] and $p = -1$) coincides with the condition (2.23) that the $N(S)$ slope be steeper than $-1.5$. For $\bar{q}_0 = 0$, equation (2.23) has more solutions than equation (3.7) (compare cols. [A] and [B] of Table 1), and some solutions in Region I will also produce a $N(S)$ slope steeper than $-1.5$. This is important because we will find that the differential form of the $N$-$S$ test requires solutions in Region I and there is no way for $\bar{q}_0 = \frac{1}{2}$ to satisfy both the differential and integrated tests simultaneously. On the other hand, for the $\bar{q}_0 = 1$ case the solutions of (3.8) overlap those of (2.23) only when $\epsilon > 0$, and then the $e$ range is very narrow.

The very existence of a maximum in $\zeta_L$ poses some problems. In such cases for given $L$ and $S$, there are two solutions of (3.2), $\varkappa_1$ and $\varkappa_2$ (where $\varkappa_1 < \varkappa_* < \varkappa_2$), and it is to be wondered why we do not observe many large $z$, especially when the corresponding space volumes are large and would contain many sources if uniformly distributed. Presumably $\zeta_L$ lumps all effects such as geometry, bolometric correction, and evolution. Since the light travel times would still be long even though $\zeta_L$ is "short," there may be focusing problems. Also $\zeta_L$ declines after its maximum slower than it rose, and a considerable region around the maximum might not be observable in present surveys; however, barring unknown effects in an infinite open universe, sources with enormous redshifts would be observable (in fact, we should reexamine Olbers's paradox). Possible explanations for their absence are:

*a*) The redshifts would be so great that the usual lines would be shifted out of the observed frequency range, or observers are looking only for patterns around $z = 4$, not $z = 20$.

*b*) The scale function $\beta^e$ is too simple to account for the variation of source density with $z$. In standard cosmology one just assumes that the evolution is turned off before $z_c$; that is, radio sources may conveniently not exist or evolve before $z_c$, where $z_1 < z_* \lesssim z_c < z_2$. One should investigate whether something interesting is occurring at that time. Any observational effect of the reheating of the intergalactic gas is clearly pertinent. In some QSO models (Rees and Setti 1968), the source is quenched before it can be observed at high intergalactic densities.

*c*) If the universe is closed and finite with a finite number of sources, we would expect to observe only a finite number of sources on one side of the antipodes.

*d*) The geometry of the universe is such that $\zeta_L$ is asymptotic to its maximum at $z_* = \infty$ and the long asymptotic region is beyond our present instruments. Several problems are: (1) $\varkappa_* = \infty$ depends on $\alpha$, which is different for different sources; (2) $\bar{q}_0 = \frac{1}{2}$ would seem to be excluded because $N$-$S$ is observed to be non-Euclidean. The choice $\bar{q}_0 \sim 0$ seems manageable for both the integrated and differential counts. The solutions $\bar{q}_0 > \frac{1}{2}$, $\varkappa_* = \infty$ may be acceptable; this is explanation (*c*) again, of course.

*e*) There may be obscuring material in the early universe. The contribution of the obscured sources to the background radiation should be calculated.

*f*) For the same $\epsilon$, $e$, $|p|$ increases with $|\alpha|$ so that flatter sources bring us farther into Region II. This may be an expression of the flattening of observed sources with redshift. The "true" ($\epsilon$, $e$) may be such that steep sources are in Region I and become progressively invisible with $z$ and flat sources are near or into Region II. If the sources

actually steepened with increasing $z$ and if the opposite observed weak correlation of flat sources with high $z$ were a selection effect, the sources at high $z$ would be invisible even though the sources' fit at low $z$ would imply some $z_* < \infty$.

We remind the reader that the absence of sources with high redshift is also an outstanding problem in the non–scale-covariant cosmology which provides fewer explanations.

## IV. THE DIFFERENTIAL COUNT

Let us first write the number of sources (per sterad) with luminosity between $L$ and $L + dL$ as

$$n(L, r)dr = R^3(t_e)(1 - kr_e^2)^{-1/2}r_e^2 dr_e \Phi(t_e, L)dL\,. \tag{4.1}$$

If in general we allow for a time variation of the number of sources, then we should write

$$n(t)R^3(t) = n_0 R_0^3 f(t)\,. \tag{4.2}$$

Then

$$n(L, r)dLdr = R_0^3(1 - kr_e^2)^{-1/2}r_e^2 dr_e \Phi(t_0, L)dL\,, \tag{4.3}$$

where $\Phi(L)$ is the radio luminosity function. Using (3.1), (3.2), (3.3), and

$$\frac{dr_e}{dz} = \left(\frac{c}{\bar{H}_0 \bar{R}_0}\right)(1 - kr_e^2)^{1/2}(1 + z)^{-1}(1 + 2\bar{q}_0 z)^{-1/2}\,,$$

and changing variables, (4.1) can now be expressed as

$$\begin{aligned} n(L, r)dLdr &= 4\pi(c/\bar{H}_0)^5\left[\frac{F^2(z, \bar{q}_0)f(t)\zeta_L^2(\beta)}{(1 + z)^3(1 + 2\bar{q}_0 z)^{1/2}}\right]\Phi(L)dSdz \\ &\equiv 4\pi(c/\bar{H}_0)^5\zeta_n^4(\beta)\Phi(L)dSdz \\ &\equiv (S, z)dSdz \end{aligned} \tag{4.4}$$

which defines $\zeta_n^4$ as the expression in the brackets. The symbols $\zeta_L$ and $\zeta_n$ have been introduced to facilitate the comparison of our results with the ones corresponding to standard cosmology as derived, for example, by von Hoerner, which can be recovered by putting $\beta = 1$, $z = z$. The exact expressions (4.4) and (3.3) constitute the basis for our future analyses.

Since, as we shall see later, the luminosity function can be written as

$$\Phi(L) \sim L^{-(n+1)}; \qquad L_m < L < L_M\,, \tag{4.5}$$

we can use (3.3) to eliminate $L$ and find the final expression for the number count normalized to the Euclidean value $n_E \sim S^{-3/2}$. Integrating $n(S, z)$ over $z$ to get $n(S)$, we obtain

$$n_n(S) \equiv \frac{n(S)}{n_E(S)} = AS^{1.5-n}\int_{z_m}^{z_M} \frac{f(t)F^2(z, \bar{q}_0)\zeta_L^{-2n}(z, \bar{q}_0, \beta)dz}{(1 + z)^3(1 + 2\bar{q}_0 z)^{1/2}}\,, \tag{4.6}$$

where

$$\begin{aligned} A &= (3 - 2n)(4\pi c^2/\bar{H}_0^2)^{1.5-n}[L_M^{1.5-n} - L_m^{1.5-n}]^{-1} \quad (n \neq 1.5) \\ &= [\ln(L_M/L_m)]^{-1} \qquad\qquad\qquad\qquad (n = 1.5)\,. \end{aligned} \tag{4.7}$$

The upper and lower limits $z_M$ and $z_m$ depend on $S$ via (3.2) once $L_M$ and $L_m$ are fixed.

The $f(t)$ which we have included accounts for number density evolution. It can be formally absorbed into the general evolutionary term $\beta^e$ (see [3.3]). We will follow this procedure and not refer to $f(t)$ again.

The solution of (3.3) and (3.2) for $z_M$ and $z_m$ must be found by iterative techniques in most cases. As $S$ becomes smaller, $\zeta_L$ increases and it becomes increasingly difficult to find the limits. As $p$ approaches Region II, $\zeta_L$ increases more slowly with $z$ and we must go to very high $z$. When $\epsilon < 0$, $z < z$, but both $z$ and $z$ can go to infinity as we approach the boundary of Region II. When we are in Region II, for some values of $L$ and $S$, $\zeta_L$ may be larger than $\zeta_L{}^*$ and there will be no solution for $z$. Since this can occur for $S$ which are no smaller than the observed values and since $L_M$ comes from the RLF (as determined within the theory from the data), an inconsistency might be suspected until it is noted that the $L_M$ calculated from the data was contributed by a datum associated with a much higher $S$ and lower $\zeta_L$ than those being used for the limits of the integral in these cases. Therefore the very low $S$ observations would be of sources with $L < L_M$, and we are allowed conceptually to lower $L_M$ for low $S$ so that $\zeta_L = \zeta_L{}^*$. When the lower limit $L_m$ and $S$ yield a $\zeta_L$ which leads to unphysical $z$'s, this procedure of lowering $L$ is not permissible

since there are no $L$ observed smaller than $L_m$; there is sufficient reason to reject the model corresponding to ($\epsilon$, $e$, $\alpha$, $\bar{q}_0$). The most obvious culprit is $\alpha$ which would be raised.

The integration was performed by (*a*) straight quadrature, (*b*) ln steps, (*c*) ln, ln steps, and (*d*) Gaussian techniques and to as many steps ($10^2$–$10^5$) as necessary, depending on the limits and function. to stabilize the results.

## V. ANALYTIC CASES

Using (3.3), we can rewrite (4.6) as

$$n_n(S) = AS^{3/2-n}\int_{x_m}^{x_M} \frac{F^{2-2n}(x, \bar{q}_0)\beta^{-2n}x(x)dx}{(1+x)^{3-n(1+\alpha)}(1+2\bar{q}_0x)^{1/2}}\,. \tag{5.1}$$

The limits $x_m$ and $x_M$ are again a solution of (3.2) and (3.3). We shall study here the cases when $\beta$ can be expressed as a simple power law of the variable $(1+x)$, i.e.,

$$\beta = (1+x)^n\,. \tag{5.2}$$

From equations (3.4) and (3.5) we derive

$$\begin{aligned} \eta &= \frac{\epsilon}{1-\epsilon} && (\bar{q}_0 = 0)\,; \\ \eta &= \frac{3\epsilon}{2(1-\epsilon)} && (\bar{q}_0 = \tfrac{1}{2})\,; \\ \eta &= \frac{\epsilon}{1-\epsilon}\frac{1}{\bar{H}_0\bar{t}_0} && (\bar{q}_0 = 1,\ \bar{H}_0\bar{t}_0 = \tfrac{1}{2}\pi - 1,\ x \sim 0)\,. \end{aligned} \tag{5.3}$$

Collecting the powers of $(1+x)$, we can rewrite (5.1) as

$$n_n(S) = AS^{3/2-n}\int_{x_m}^{x_M} F^{2-2n}(\bar{q}_0, x)(1+x)^{-3-2np}(1+2\bar{q}_0x)^{-1/2}dx\,, \tag{5.4}$$

where $p$ is the same as that given by (3.7). Instead of specifying the parameters $x(g, \alpha, e)$ and $\epsilon$ separately, we shall discuss global cases corresponding to specific values of $p$ (which arise from many combinations of the parameters $\bar{q}_0$, $\epsilon$, $e$, and $\alpha$) and $\bar{q}_0$. For convenience we shall use (3.2) to define

$$\zeta_L = \bar{H}_0c^{-1}\left(\frac{L_0}{4\pi S}\right)^{1/2} \equiv \Lambda\,. \tag{5.5}$$

We present below the following cases: for $\bar{q}_0 = 0$: $n = 1$ (all $p$) and $n = 2$ ($p = -1$). For $\bar{q}_0 = \frac{1}{2}$: $n = 1$ ($p = -2, -\frac{7}{4}, -\frac{4}{3}, -1, -\frac{1}{2}, -\frac{1}{4}$, and 0) and $n = 1.5$ ($p = -\frac{4}{3}$). We also have treated analytically the $\bar{q}_0 = \frac{1}{2}$ cases $n = 1.5$ ($p = -\frac{3}{2}, -\frac{7}{6}, -1, -\frac{5}{6}$, and $-\frac{2}{3}$) and $n = 2$ ($p = -\frac{5}{4}, -\frac{9}{8}, -1, -\frac{7}{8}$, and $-\frac{3}{4}$) but do not present them here for simple reasons of space and because the reader after seeing the first few cases will be able easily to do these and many others himself.

### *a) Case A:* $\bar{q}_0 = \frac{1}{2}$, $p = -1$

In this case of zero curvature, $\bar{H}_0\bar{t}_0 = \frac{2}{3}$, we have from equation (3.6b)

$$F(x, \bar{q}_0) = 2[1 + x - (1+x)^{1/2}]\,. \tag{5.6}$$

Using (3.5), we have

$$\zeta_L = 2[1 - (1+x)^{-1/2}] \tag{5.6a}$$

or

$$1 + x_{m,M} = (1 - \tfrac{1}{2}\Lambda_{m,M})^{-2}\,. \tag{5.6b}$$

Substituting (5.6) in (5.4), we obtain

$$n_n = AS^{3/2-n}\int_{x_m}^{x_M} 2^{2-2n}(1+x)^{2n-3.5}[1 + x - (1+x)^{1/2}]^{2-2n}dx\,. \tag{5.7}$$

If $n = 1$, using (4.7) we find that $A = S^{-1/2}[\Lambda_M - \Lambda_m]^{-1}$ and

$$n_n = AS^{1/2}\int_{x_M}^{x_m}(1 + x)^{-1.5}dx = 1\,; \tag{5.8}$$

i.e., the model makes the same predictions as the Euclidean model.

Similarly, if $n = 1.5$ and if we change variables to $y = (1 + x)^{1/2}$,

$$n_n = A\int_{y_m}^{y_M}\frac{dy}{y(y-1)} = 1\,. \tag{5.9}$$

Again, if $n = 2$, equation (4.7) becomes $A = S^{1/2}[\Lambda_m{}^{-1} - \Lambda_M{}^{-1}]^{-1}$ and we find, with the same change of variables,

$$n_n = \tfrac{1}{2}AS^{-1/2}\int_{y_m}^{y_M}\frac{dy}{(y-1)^2} = 1\,, \tag{5.10}$$

which is once more independent of $S$ and $L_0$.

In general for $\bar{q}_0 = \frac{1}{2}$ and for any $(g, e, \alpha)$ which gives $p = -1$, the result is Euclidean and $x_* = \infty$. The value $p = -1$ when $\bar{q}_0 = \frac{1}{2}$ corresponds to the boundary between Regions I and II, and the $e$ values which will give this Euclidean result are shown as a function of $\epsilon$ for various $\alpha$ in Figure 1*b* and listed for $\alpha = -0.75$ in column (B) of Table I. When these are multiplied by column (D), we obtain the corresponding $E$ values if we write

$$L = L_0\beta^e = L_0(1 + z)^E\,. \tag{5.11}$$

*b) Case B, $\bar{q}_0 = 0$*

For $\bar{q}_0 = 0$, we have $\bar{t}_0\bar{H}_0 = 1$:

$$F = x(1 + x/2) \tag{5.12}$$

and

$$\zeta_L = F(1 + 2F)^{p/2} \tag{5.13}$$

with

$$1 + x = (1 + 2F)^{1/2}\,. \tag{5.14}$$

Substitution in (5.2) yields

$$n_n = AS^{3/2-n}\int F^{2-2n}(1 + 2F)^{-2-np}dF\,. \tag{5.15}$$

(B1) If $p = -2/n$,

$$n_n(S) = \frac{AS^{3/2-n}}{3 - 2n}\,[F^{3-2n}(x)]_{x_m}^{x_M}$$

and

$$\Lambda = F(1 + 2F)^{-1/n}\,.$$

(B2) A particular case of case B1 is $n = 1$ $(p = -2)$, $F = \Lambda/(1 - 2\Lambda)$, and the upper limit $\Lambda_M$ corresponds to $x_M = \infty$. $A$ is given by (4.7), as already found in case A. Then

$$\begin{aligned} n_n(S) &= \left(\frac{\Lambda_M}{1 - 2\Lambda_M} - \frac{\Lambda_m}{1 - 2\Lambda_m}\right)\frac{1}{(\Lambda_M - \Lambda_m)} \\ &= \left[\frac{L_M{}^{1/2}}{1 - \bar{H}_0c^{-1}(L_M/\pi S)^{1/2}} - \frac{L_m{}^{1/2}}{1 - \bar{H}_0c^{-1}(L_m/\pi S)^{1/2}}\right]\left(\frac{1}{L_M{}^{1/2} - L_m{}^{1/2}}\right), \end{aligned} \tag{5.16}$$

which is a function of $S$ and depends on the limits $L_M$ and $L_m$ of the RLF. The values of $e$ satisfying this case are given as a function of $\epsilon$ for various spectral indices in Figure 1*a* and tabulated for $\alpha = -0.75$ in column B of Table 1 for $\bar{q}_0 = 0$. We are again on the boundary between Regions I and II.

(B3) Another subcase of B1 is: $n = 2$, $p = -1$:

$$F = \Lambda[1 + (1 + \Lambda^2)^{1/2}]\,,$$

$$n_n(S) = \left[\frac{L_m{}^{1/2}}{1 + (1 + \bar{H}_0{}^2c^{-2}L_M/4\pi S)^{1/2}} - \frac{L_M{}^{1/2}}{1 + (1 + \bar{H}_0{}^2c^{-2}L_m/4\pi S)^{1/2}}\right]\left(\frac{1}{L_M{}^{1/2} - L_m{}^{1/2}}\right).$$

This again depends on $S$, $L_M$, and $L_m$. We are in Region I.

(B4) If $n = 1$, $p \neq -1, -2$, then

$$1 + 2F = (1 - 2\Lambda)^{-1} \tag{5.17}$$

and

$$n_n(S) = \frac{(1 - 2\Lambda_M)^{p+1} - (1 - 2\Lambda)_m^{p+1}}{(\Lambda_M - \Lambda_m)(-2p - 2)} . \tag{5.17a}$$

This expression is exact in both Regions I and II as long as $p \neq -1, -2$.

(B5) If $p = -2$ and $n = 1$, this case is the boundary case B2.

(B6) If $p = -1$ and $n = 1$,

$$n_n(S) = \tfrac{1}{2}\Lambda S^{1/2} \ln \frac{1 - (2\bar{H}_0/c)(L_m/4\pi S)^{1/2}}{1 - (2\bar{H}_0/c)(L_m/4\pi S)^{1/2}} . \tag{5.18}$$

This case corresponds to Region I. It has a flatter RLF than case B3; consequently the graph of $\log n$ versus $\log S$ appears more curved.

*c) Case C:* $\bar{q}_0 = \frac{1}{2}, p = -2, n = 1$

Again we are in Region II. We find

$$n_n(S) = \frac{2}{3} \frac{(1 + z_M)^{3/2} - (1 + z_m)^{3/2}}{\Lambda_M - \Lambda_m} , \tag{5.19}$$

where the limits are given by

$$\tfrac{1}{2}\Lambda = (1 + z)^{-1} - (1 + z)^{-3/2} , \tag{5.19a}$$

which is easily solvable by cubic methods.

*d) Case D:* $\bar{q}_0 = \frac{1}{2}, p = -\frac{1}{4}, n = 1$

Here we are in the more conventional Region I. We easily find from (5.2) that

$$n_n(S) = \frac{1}{2} \frac{(1 + z_m)^{-2} - (1 + z_M)^{-2}}{\Lambda_M - \Lambda_m} , \tag{5.20}$$

where the limits are obtained from

$$\tfrac{1}{2}\Lambda = (1 + z)^{3/4} - (1 + z)^{1/4} , \tag{5.20a}$$

which is an easily solvable cubic equation in the variable $(1 + z)^{1/4}$.

*e) Case E:* $\bar{q}_0 = \frac{1}{2}, p = -\frac{1}{2}, n = 1$

We are again in Region I. Equation (5.2) reduces to

$$n_n(S) = \frac{2}{3} \frac{(1 + \Lambda_m)^{-3} - (1 + \Lambda_M)^{-3}}{\Lambda_M - \Lambda_m} \tag{5.21}$$

since

$$\tfrac{1}{2}\Lambda = (1 + z)^{1/2} - 1 . \tag{5.21a}$$

*f) Case F:* $\bar{q}_0 = \frac{1}{2}, p = 0, n = 1$

We are in Region I and

$$n_n(S) = \frac{2}{5} \frac{(1 + z_m)^{-5/2} - (1 + z_M)^{-5/2}}{\Lambda_M - \Lambda_m} , \tag{5.22}$$

where

$$2(1 + z) = 1 + (1 + 2\Lambda)^{1/2} . \tag{5.22a}$$

*g) Case G:* $\bar{q}_0 = \frac{1}{2}, p = -\frac{4}{3}, n = 1.5$

We are in Region I, and the result is

$$n_n(S) = \frac{\ln [(1 + x_M^3)/(1 + x_m^3)]}{\ln (L_M/L_m)}, \tag{5.23}$$

where

$$\tfrac{1}{2}\Lambda = x^2 - x^5. \tag{5.23a}$$

*h) Case H:* $\bar{q}_0 = \frac{1}{2}, p = -1.75, n = 1$

We are in Region II and

$$n_n(S) = \frac{\varkappa_M - \varkappa_m}{\Lambda_M - \Lambda_m}, \tag{5.24}$$

where $\varkappa_M$ and $\varkappa_m$ are solutions of

$$\tfrac{1}{2}\Lambda = (1 + \varkappa)^{-3/4} - (1 + \varkappa)^{-5/4}. \tag{5.24a}$$

## VI. THE RADIO LUMINOSITY FUNCTION

It is our purpose to show what scale covariance can accomplish with respect to the standard theory. If we fit the data by some special artifice in evolutionary and selection functions where the standard theory uses its own artifices, the separate contributions of the two theories are obscured. For this reason we fit the simplest RLF in conformity with previous practice, namely a truncated power law

$$\varphi = CL^{-n}, \quad L_{\min} < L < L_{\max}$$
$$= 0, \qquad L_{\min} > L > L_{\max},$$

where $\varphi$ is the number of sources per unit volume with luminosities between $L$ and $10L$, which is related to $\Phi$, the number of sources per unit volume with luminosities between $L$ and $L + dL$ and

$$\Phi \sim L^{-n-1} \equiv L^{\gamma},$$

with the same limits (eq. [4.5]).

The standard methods of calculating the RLF as outlined by Petrosian (1969) were used. The first method entails calculating the absolute luminosity $L$ within the theory using equations (3.2), (3.3), and (2.2). We use the best spectral index available for each source. When this is accomplished, the largest and smallest $L$ become the limits used. At the same time the maximum redshift $z_M$ at which the source luminosity could be observed at the flux limit of the survey ($2J_\nu$) is calculated; since $\beta(z_M)$ is not known until $z_M$ is known, an iterative routine must be used in general; we used our own, Wegstein's, Newton's, and Mueller's (the same as used in finding the limits of the integral for $n_n$), finding our own most convenient for $\epsilon = -1$ and Wegstein's for $\epsilon \geq -\frac{1}{2}$. Since $\alpha$ differs from source to source for the same ($\epsilon$, $e$), some sources have a maximum in $\zeta_L$ while others do not. When there is a maximum at $\varkappa_* < \infty$, there are two solutions for $z_M$, viz., $z(M_1)$ and $z(M_2)$. The interest in finding $z_M$ is to know the volume in which the source could be observed. If the sources are uniformly distributed and the universe is open, the observable volume is infinite when there is a maximum in $\zeta_L$ and a suitable number to represent infinity to a computer is chosen. If we are in Region II and the sources are uniformly distributed but the universe is closed, the appropriate closed volume must be used. If we assume that sources do not appear before $z = 4$, we may use the volume up to the first $z(M_1)$ and add to it the volume between the second $z(M_2)$ and $z = 4$. Since, however, we do not believe in models with $\zeta_{L_*}$ at $z_* < 2$, it is unlikely that we will investigate a model with $z(M_2) < 4$, so it is sufficient to take volumes from $z = 0$ to $z = z(M_1)$. We would do this even if we were trying to simulate selection effect (*a*) in § IV.

The volumes in our theory are derived below (see also Paper III, § XII).

The Robertson-Walker metric in atomic units is

$$ds^2 = c^2dt^2 - R^2(t)[dr^2/(1 - kr^2) + r^2d\Omega^2] = c^2dt^2 - R^2(t)[d\chi^2 + \Sigma^2(\chi)d\Omega^2], \tag{6.1}$$

where

$$r = \Sigma(\chi) = \mathcal{S}[\sqrt{(-k)}\chi]/\sqrt{(-k)} = \sinh^{-1}[\sqrt{(-k}\chi]/\sqrt{(-k)} \tag{6.2}$$

and

$$d\chi = \frac{dr}{(1 - kr^2)^{1/2}}.$$

For photons $ds = 0$ and if $d\Omega = 0$ for convenience,

$$d\chi = \frac{cdt}{R(t)}, \tag{6.3a}$$

1979ApJS...41..301C

TABLE 3

| | (ϵ,e) = (-1.00, -3.50) $\bar{q}_o$=0 | | | | (ϵ,e) = (-0.50, -4.50) $\bar{q}_o$=0 | | | | (ϵ,e) = (0.50, -1.25) $\bar{q}_o$ = 0.50 | | | | (ϵ,e) = (0.92, -1.40) $\bar{q}_o$ = 1.00 | | | |
|---|---|---|---|---|---|---|---|---|---|---|---|---|---|---|---|---|
| Z | $\bar{z}$ | LOG L | V(MPC3) | VM(MPC3) | $\bar{z}$ | LOG L | V(MPC3) | VM(MPC3) | $\bar{z}$ | LOG L | V(MPC3) | VM(MPC3) | $\bar{z}$ | LOG L | V(MPC3) | VM(MPC3) |
| 0.02 | 0.051 | 25.5 | .136D+08 | .234D+09 | 0.039 | 25.5 | .136D+08 | .231D+09 | 0.010 | 25.5 | .135D+08 | .222D+09 | 0.001 | 25.5 | .136D+08 | .223D+09 |
| 0.03 | 0.053 | 25.9 | .153D+08 | .865D+09 | 0.039 | 25.9 | .153D+08 | .845D+09 | 0.010 | 25.9 | .152D+08 | .799D+09 | 0.001 | 25.9 | .153D+08 | .792D+09 |
| 0.06 | 0.113 | 26.5 | .139D+09 | .893D+10 | 0.084 | 26.5 | .139D+09 | .858D+10 | 0.022 | 26.5 | .137D+09 | .753D+10 | 0.003 | 26.6 | .138D+09 | .755D+10 |
| 0.07 | 0.134 | 26.1 | .227D+09 | .179D+10 | 0.099 | 26.1 | .226D+09 | .175D+10 | 0.026 | 26.1 | .222D+09 | .164D+10 | 0.003 | 26.1 | .225D+09 | .166D+10 |
| 0.07 | 0.141 | 26.0 | .259D+09 | .130D+10 | 0.104 | 26.0 | .258D+09 | .128D+10 | 0.027 | 26.0 | .253D+09 | .121D+10 | 0.003 | 26.0 | .257D+09 | .123D+10 |
| 0.08 | 0.164 | 25.9 | .400D+09 | .928D+09 | 0.121 | 25.9 | .399D+09 | .920D+09 | 0.031 | 26.0 | .389D+09 | .880D+09 | 0.004 | 26.0 | .396D+09 | .895D+09 |
| 0.08 | 0.171 | 27.1 | .445D+09 | .661D+11 | 0.125 | 27.1 | .444D+09 | .631D+11 | 0.032 | 27.1 | .433D+09 | .510D+11 | 0.004 | 27.1 | .441D+09 | .510D+11 |
| 0.10 | 0.206 | 26.2 | .745D+09 | .225D+10 | 0.151 | 26.2 | .742D+09 | .222D+10 | 0.038 | 26.2 | .719D+09 | .209D+10 | 0.004 | 26.2 | .736D+09 | .213D+10 |
| 0.11 | 0.228 | 26.6 | .984D+09 | .110D+11 | 0.166 | 26.6 | .981D+09 | .107D+11 | 0.042 | 26.6 | .946D+09 | .947D+10 | 0.005 | 26.6 | .971D+09 | .964D+10 |
| 0.12 | 0.252 | 26.8 | .130D+10 | .218D+11 | 0.184 | 26.8 | .129D+10 | .211D+11 | 0.046 | 26.8 | .124D+10 | .182D+11 | 0.005 | 26.8 | .128D+10 | .185D+11 |
| 0.13 | 0.277 | 26.8 | .167D+10 | .188D+11 | 0.201 | 26.8 | .166D+10 | .183D+11 | 0.050 | 26.8 | .159D+10 | .159D+11 | 0.006 | 26.8 | .164D+10 | .163D+11 |
| 0.14 | 0.293 | 27.0 | .194D+10 | .440D+11 | 0.212 | 27.0 | .193D+10 | .425D+11 | 0.053 | 27.0 | .184D+10 | .356D+11 | 0.006 | 27.0 | .190D+10 | .363D+11 |
| 0.15 | 0.327 | 26.9 | .260D+10 | .355D+11 | 0.236 | 26.9 | .259D+10 | .344D+11 | 0.058 | 26.9 | .246D+10 | .292D+11 | 0.007 | 27.0 | .254D+10 | .299D+11 |
| 0.16 | 0.341 | 27.8 | .291D+10 | .108D+13 | 0.246 | 27.8 | .288D+10 | .114D+13 | 0.060 | 27.8 | .273D+10 | .989D+12 | 0.007 | 27.8 | .283D+10 | .912D+12 |
| 0.16 | 0.348 | 27.0 | .306D+10 | .564D+11 | 0.251 | 27.0 | .304D+10 | .546D+11 | 0.062 | 27.1 | .288D+10 | .455D+11 | 0.007 | 27.1 | .299D+10 | .465D+11 |
| 0.17 | 0.362 | 26.9 | .340D+10 | .367D+11 | 0.261 | 26.9 | .337D+10 | .356D+11 | 0.064 | 27.0 | .318D+10 | .303D+11 | 0.007 | 27.0 | .330D+10 | .311D+11 |
| 0.18 | 0.404 | 27.5 | .453D+10 | .268D+12 | 0.290 | 27.5 | .448D+10 | .263D+12 | 0.070 | 27.6 | .421D+10 | .206D+12 | 0.008 | 27.6 | .438D+10 | .210D+12 |
| 0.19 | 0.418 | 26.6 | .495D+10 | .169D+11 | 0.300 | 26.6 | .490D+10 | .165D+11 | 0.072 | 26.7 | .459D+10 | .146D+11 | 0.008 | 26.7 | .479D+10 | .151D+11 |
| 0.20 | 0.430 | 27.3 | .532D+10 | .937D+11 | 0.308 | 27.3 | .526D+10 | .907D+11 | 0.074 | 27.3 | .492D+10 | .741D+11 | 0.009 | 27.3 | .514D+10 | .767D+11 |
| 0.20 | 0.440 | 27.2 | .563D+10 | .106D+12 | 0.315 | 27.2 | .557D+10 | .103D+12 | 0.076 | 27.3 | .519D+10 | .842D+11 | 0.009 | 27.3 | .543D+10 | .866D+11 |
| 0.20 | 0.440 | 27.3 | .563D+10 | .160D+12 | 0.315 | 27.3 | .557D+10 | .156D+12 | 0.076 | 27.4 | .519D+10 | .125D+12 | 0.009 | 27.4 | .543D+10 | .128D+12 |
| 0.21 | 0.476 | 27.4 | .689D+10 | .152D+12 | 0.339 | 27.4 | .680D+10 | .149D+12 | 0.081 | 27.4 | .630D+10 | .119D+12 | 0.009 | 27.4 | .661D+10 | .123D+12 |
| 0.24 | 0.535 | 27.3 | .924D+10 | .117D+12 | 0.379 | 27.3 | .909D+10 | .114D+12 | 0.090 | 27.3 | .835D+10 | .929D+11 | 0.010 | 27.3 | .880D+10 | .966D+11 |
| 0.24 | 0.538 | 26.6 | .935D+10 | .109D+11 | 0.381 | 26.6 | .920D+10 | .107D+11 | 0.090 | 26.6 | .845D+10 | .980D+10 | 0.010 | 26.6 | .890D+10 | .103D+11 |
| 0.24 | 0.538 | 27.0 | .935D+10 | .405D+11 | 0.381 | 27.0 | .920D+10 | .393D+11 | 0.090 | 27.0 | .845D+10 | .337D+11 | 0.010 | 27.0 | .890D+10 | .353D+11 |
| 0.25 | 0.560 | 26.7 | .103D+11 | .156D+11 | 0.396 | 26.7 | .102D+11 | .153D+11 | 0.093 | 26.7 | .931D+10 | .138D+11 | 0.011 | 26.7 | .983D+10 | .145D+11 |
| 0.26 | 0.578 | 27.7 | .112D+11 | .458D+12 | 0.408 | 27.7 | .110D+11 | .454D+12 | 0.095 | 27.7 | .100D+11 | .352D+12 | 0.011 | 27.7 | .106D+11 | .364D+12 |
| 0.26 | 0.588 | 26.9 | .117D+11 | .337D+11 | 0.414 | 26.9 | .114D+11 | .328D+11 | 0.097 | 26.9 | .104D+11 | .284D+11 | 0.011 | 26.9 | .110D+11 | .298D+11 |
| 0.26 | 0.593 | 27.3 | .122D+11 | .144D+12 | 0.421 | 27.3 | .119D+11 | .141D+12 | 0.098 | 27.4 | .108D+11 | .114D+12 | 0.011 | 27.4 | .115D+11 | .119D+12 |
| 0.27 | 0.605 | 26.7 | .125D+11 | .135D+11 | 0.426 | 26.7 | .123D+11 | .132D+11 | 0.099 | 26.7 | .112D+11 | .120D+11 | 0.011 | 26.8 | .118D+11 | .127D+11 |
| 0.27 | 0.618 | 27.6 | .132D+11 | .317D+12 | 0.435 | 27.6 | .129D+11 | .313D+12 | 0.101 | 27.6 | .117D+11 | .246D+12 | 0.011 | 27.6 | .124D+11 | .255D+12 |
| 0.30 | 0.685 | 26.8 | .170D+11 | .225D+11 | 0.479 | 26.8 | .166D+11 | .219D+11 | 0.110 | 26.8 | .149D+11 | .194D+11 | 0.012 | 26.9 | .158D+11 | .206D+11 |
| 0.30 | 0.698 | 26.7 | .177D+11 | .177D+11 | 0.487 | 26.7 | .173D+11 | .173D+11 | 0.112 | 26.8 | .155D+11 | .155D+11 | 0.013 | 26.8 | .165D+11 | .165D+11 |
| 0.31 | 0.706 | 27.7 | .182D+11 | .576D+12 | 0.493 | 27.7 | .178D+11 | .577D+12 | 0.113 | 27.8 | .159D+11 | .451D+12 | 0.013 | 27.8 | .170D+11 | .467D+12 |
| 0.31 | 0.719 | 27.5 | .190D+11 | .234D+12 | 0.501 | 27.5 | .186D+11 | .229D+12 | 0.114 | 27.5 | .166D+11 | .182D+12 | 0.013 | 27.5 | .177D+11 | .191D+12 |
| 0.32 | 0.742 | 27.4 | .206D+11 | .218D+12 | 0.517 | 27.4 | .200D+11 | .214D+12 | 0.117 | 27.4 | .178D+11 | .172D+12 | 0.013 | 27.5 | .191D+11 | .180D+12 |
| 0.32 | 0.750 | 27.3 | .211D+11 | .139D+12 | 0.522 | 27.3 | .206D+11 | .135D+12 | 0.118 | 27.3 | .182D+11 | .110D+12 | 0.013 | 27.4 | .195D+11 | .116D+12 |
| 0.33 | 0.780 | 27.2 | .231D+11 | .109D+12 | 0.541 | 27.2 | .225D+11 | .106D+12 | 0.122 | 27.3 | .199D+11 | .867D+11 | 0.014 | 27.3 | .213D+11 | .920D+11 |
| 0.34 | 0.806 | 27.5 | .251D+11 | .216D+12 | 0.558 | 27.5 | .243D+11 | .211D+12 | 0.126 | 27.5 | .214D+11 | .167D+12 | 0.014 | 27.5 | .230D+11 | .177D+12 |
| 0.36 | 0.852 | 27.5 | .286D+11 | .267D+12 | 0.583 | 27.5 | .276D+11 | .261D+12 | 0.131 | 27.6 | .242D+11 | .205D+12 | 0.015 | 27.6 | .261D+11 | .218D+12 |
| 0.36 | 0.852 | 26.9 | .286D+11 | .588D+11 | 0.588 | 27.0 | .276D+11 | .569D+11 | 0.131 | 27.0 | .242D+11 | .481D+11 | 0.015 | 27.0 | .261D+11 | .514D+11 |
| 0.37 | 0.869 | 27.6 | .299D+11 | .400D+12 | 0.598 | 27.6 | .289D+11 | .396D+12 | 0.133 | 27.6 | .252D+11 | .310D+12 | 0.015 | 27.7 | .272D+11 | .327D+12 |
| 0.37 | 0.869 | 27.0 | .299D+11 | .757D+11 | 0.598 | 27.0 | .289D+11 | .733D+11 | 0.133 | 27.1 | .252D+11 | .613D+11 | 0.015 | 27.1 | .272D+11 | .654D+11 |
| 0.37 | 0.869 | 28.3 | .299D+11 | .276D+13 | 0.598 | 28.3 | .289D+11 | .277D+13 | 0.133 | 28.3 | .252D+11 | .206D+13 | 0.015 | 28.4 | .272D+11 | .219D+13 |
| 0.37 | 0.877 | 27.3 | .306D+11 | .114D+12 | 0.604 | 27.3 | .295D+11 | .110D+12 | 0.134 | 27.3 | .257D+11 | .896D+11 | 0.015 | 27.3 | .278D+11 | .961D+11 |
| 0.37 | 0.880 | 27.7 | .309D+11 | .559D+12 | 0.605 | 27.7 | .297D+11 | .557D+12 | 0.135 | 27.7 | .259D+11 | .436D+12 | 0.015 | 27.8 | .279D+11 | .458D+12 |
| 0.37 | 0.880 | 27.6 | .308D+11 | .427D+12 | 0.605 | 27.6 | .297D+11 | .424D+12 | 0.135 | 27.6 | .259D+11 | .334D+12 | 0.015 | 27.7 | .279D+11 | .351D+12 |
| 0.38 | 0.918 | 27.0 | .340D+11 | .544D+11 | 0.630 | 27.0 | .328D+11 | .524D+11 | 0.139 | 27.1 | .284D+11 | .443D+11 | 0.016 | 27.1 | .307D+11 | .478D+11 |
| 0.39 | 0.927 | 27.5 | .347D+11 | .283D+12 | 0.635 | 27.5 | .335D+11 | .279D+12 | 0.140 | 27.5 | .289D+11 | .222D+12 | 0.016 | 27.5 | .313D+11 | .235D+12 |
| 0.41 | 0.977 | 27.4 | .393D+11 | .193D+12 | 0.667 | 27.4 | .377D+11 | .188D+12 | 0.146 | 27.4 | .323D+11 | .150D+12 | 0.016 | 27.4 | .351D+11 | .161D+12 |
| 0.41 | 0.982 | 27.5 | .393D+11 | .214D+12 | 0.671 | 27.5 | .382D+11 | .208D+12 | 0.147 | 27.5 | .327D+11 | .165D+12 | 0.016 | 27.5 | .356D+11 | .177D+12 |
| 0.41 | 0.991 | 27.7 | .406D+11 | .401D+12 | 0.676 | 27.7 | .389D+11 | .390D+12 | 0.148 | 27.7 | .333D+11 | .299D+12 | 0.016 | 27.8 | .362D+11 | .322D+12 |
| 0.42 | 1.016 | 27.4 | .430D+11 | .144D+12 | 0.692 | 27.4 | .412D+11 | .138D+12 | 0.151 | 27.4 | .351D+11 | .111D+12 | 0.017 | 27.4 | .383D+11 | .120D+12 |
| 0.43 | 1.031 | 29.1 | .444D+11 | .155D+13 | 0.701 | 28.2 | .425D+11 | .153D+13 | 0.152 | 28.2 | .362D+11 | .112D+13 | 0.017 | 28.2 | .394D+11 | .121D+13 |

TABLE 3A

| | (ϵ,e) = (-1.00, -3.50) $\bar{q}_o$=0 | | | | (ϵ,e) = (-0.50, -4.50) $\bar{q}_o$=0 | | | | (ϵ,e) = (0.50, -1.25) $\bar{q}_o$ = 0.50 | | | | (ϵ,e) = (0.92, -1.40) $\bar{q}_o$ = 1.00 | | | |
|---|---|---|---|---|---|---|---|---|---|---|---|---|---|---|---|---|
| Z | $\bar{z}$ | LOG L | V(MPC3) | VM(MPC3) | $\bar{z}$ | LOG L | V(MPC3) | VM(MPC3) | $\bar{z}$ | LOG L | V(MPC3) | VM(MPC3) | $\bar{z}$ | LOG L | V(MPC3) | VM(MPC3) |
| 1.02 | 3.088 | 28.3 | .468D+12 | .269D+13 | 1.875 | 28.2 | .394D+12 | .237D+13 | 0.325 | 28.2 | .256D+12 | .154D+13 | 0.034 | 28.3 | .304D+12 | .180D+13 |
| 1.03 | 3.117 | 28.4 | .476D+12 | .622D+13 | 1.890 | 28.4 | .401D+12 | .570D+13 | 0.327 | 28.4 | .260D+12 | .481D+13 | 0.034 | 28.4 | .308D+12 | .488D+13 |
| 1.04 | 3.149 | 28.0 | .486D+12 | .226D+13 | 1.907 | 28.0 | .409D+12 | .206D+13 | 0.329 | 27.9 | .264D+12 | .154D+13 | 0.034 | 28.0 | .314D+12 | .170D+13 |
| 1.04 | 3.149 | 28.5 | .486D+12 | .682D+13 | 1.907 | 28.4 | .409D+12 | .625D+13 | 0.329 | 28.4 | .264D+12 | .501D+13 | 0.034 | 28.4 | .314D+12 | .538D+13 |
| 1.05 | 3.223 | 28.1 | .510D+12 | .258D+13 | 1.946 | 28.0 | .426D+12 | .233D+13 | 0.334 | 28.0 | .273D+12 | .17CD+13 | 0.035 | 28.1 | .325D+12 | .189D+13 |
| 1.06 | 3.256 | 28.6 | .520D+12 | .542D+13 | 1.963 | 28.6 | .434D+12 | .461D+13 | 0.336 | 28.6 | .277D+12 | .265D+13 | 0.035 | 28.6 | .330D+12 | .322D+13 |
| 1.06 | 3.256 | 28.6 | .520D+12 | .544D+13 | 1.963 | 28.5 | .434D+12 | .467D+13 | 0.336 | 28.5 | .277D+12 | .277D+13 | 0.035 | 28.6 | .330D+12 | .333D+13 |
| 1.08 | 3.335 | 27.8 | .546D+12 | .799D+12 | 2.004 | 27.7 | .454D+12 | .674D+12 | 0.341 | 27.7 | .287D+12 | .428D+12 | 0.035 | 27.8 | .343D+12 | .507D+12 |
| 1.09 | 3.360 | 27.8 | .554D+12 | .631D+12 | 2.017 | 27.8 | .460D+12 | .526D+12 | 0.342 | 27.7 | .290D+12 | .331D+12 | 0.036 | 27.8 | .347D+12 | .395D+12 |
| 1.11 | 3.452 | 28.4 | .585D+12 | .519D+13 | 2.065 | 28.3 | .483D+12 | .463D+13 | 0.348 | 28.3 | .302D+12 | .340D+13 | 0.036 | 28.3 | .362D+12 | .378D+13 |
| 1.11 | 3.452 | 28.7 | .585D+12 | .832D+13 | 2.065 | 28.7 | .483D+12 | .703D+13 | 0.348 | 28.7 | .302D+12 | .398D+13 | 0.036 | 28.7 | .362D+12 | .487D+13 |
| 1.11 | 3.461 | 28.5 | .588D+12 | .401D+13 | 2.069 | 28.4 | .485D+12 | .340D+13 | 0.349 | 28.4 | .303D+12 | .202D+13 | 0.036 | 28.5 | .363D+12 | .243D+13 |
| 1.12 | 3.494 | 27.8 | .600D+12 | .871D+12 | 2.087 | 27.8 | .494D+12 | .727D+12 | 0.351 | 27.7 | .307D+12 | .453D+12 | 0.036 | 27.8 | .369D+12 | .540D+12 |
| 1.14 | 3.580 | 27.9 | .629D+12 | .119D+13 | 2.131 | 27.8 | .516D+12 | .100D+13 | 0.356 | 27.8 | .318D+12 | .628D+12 | 0.037 | 27.9 | .382D+12 | .744D+12 |
| 1.19 | 3.783 | 27.9 | .703D+12 | .34CD+13 | 2.234 | 27.9 | .570D+12 | .318D+13 | 0.368 | 27.8 | .344D+12 | .113D+15 | 0.038 | 27.9 | .416D+12 | .352D+13 |
| 1.25 | 4.058 | 28.2 | .808D+12 | .351D+13 | 2.373 | 28.2 | .646D+12 | .297D+13 | 0.383 | 28.1 | .379D+12 | .192D+13 | 0.039 | 28.2 | .461D+12 | .223D+13 |
| 1.25 | 4.081 | 28.2 | .817D+12 | .173D+13 | 2.384 | 28.1 | .652D+12 | .140D+13 | 0.384 | 28.1 | .382D+12 | .8C9D+12 | 0.039 | 28.1 | .465D+12 | .581D+12 |
| 1.33 | 4.415 | 28.3 | .956D+12 | .668D+13 | 2.550 | 28.3 | .749D+12 | .579D+13 | 0.402 | 28.2 | .425D+12 | .515D+13 | 0.041 | 28.3 | .521D+12 | .516D+13 |
| 1.38 | 4.674 | 28.8 | .107D+13 | .991D+13 | 2.676 | 28.7 | .828D+12 | .779D+13 | 0.415 | 28.7 | .458D+12 | .40CD+13 | 0.042 | 28.7 | .564D+12 | .502D+13 |
| 1.40 | 4.760 | 28.7 | .111D+13 | .784D+13 | 2.718 | 28.6 | .854D+12 | .621D+13 | 0.419 | 28.5 | .469D+12 | .337D+13 | 0.042 | 28.6 | .579D+12 | .415D+13 |
| 1.40 | 4.765 | 28.0 | .111D+13 | .119D+13 | 2.720 | 27.9 | .856D+12 | .917D+12 | 0.420 | 27.8 | .469D+12 | .503D+12 | 0.042 | 27.9 | .580D+12 | .621D+12 |
| 1.40 | 4.765 | 28.0 | .111D+13 | .333D+13 | 2.720 | 27.9 | .856D+12 | .282D+13 | 0.420 | 27.8 | .469D+12 | .233D+13 | 0.042 | 27.9 | .580D+12 | .238D+13 |
| 1.40 | 4.774 | 28.8 | .112D+13 | .221D+14 | 2.725 | 28.7 | .859D+12 | .188D+14 | 0.420 | 28.6 | .471D+12 | .227D+14 | 0.043 | 28.7 | .581D+12 | .187D+14 |
| 1.44 | 4.949 | 29.4 | .120D+13 | .520D+14 | 2.809 | 29.4 | .914D+12 | .387D+14 | 0.429 | 29.3 | .493D+12 | .147D+14 | 0.043 | 29.3 | .611D+12 | .208D+14 |
| 1.44 | 4.973 | 28.3 | .121D+13 | .260D+13 | 2.821 | 28.2 | .922D+12 | .202D+13 | 0.430 | 28.2 | .496D+12 | .167D+13 | 0.043 | 28.2 | .615D+12 | .133D+13 |
| 1.45 | 4.978 | 28.4 | .121D+13 | .563D+13 | 2.823 | 28.3 | .923D+12 | .454D+13 | 0.430 | 28.2 | .496D+12 | .282D+13 | 0.043 | 28.3 | .616D+12 | .331D+13 |
| 1.52 | 5.345 | 28.9 | .139D+13 | .129D+14 | 2.993 | 28.8 | .104D+13 | .984D+13 | 0.447 | 28.7 | .543D+12 | .499D+13 | 0.045 | 28.7 | .679D+12 | .628D+13 |
| 1.52 | 5.360 | 28.1 | .140D+13 | .140D+13 | 3.005 | 28.0 | .105D+13 | .105D+13 | 0.448 | 27.9 | .545D+12 | .545D+12 | 0.045 | 28.0 | .681D+12 | .681D+12 |
| 1.53 | 5.421 | 28.9 | .143D+13 | .139D+14 | 3.034 | 28.8 | .107D+13 | .106D+14 | 0.451 | 28.7 | .553D+12 | .63CD+13 | 0.045 | 28.8 | .692D+12 | .669D+13 |
| 1.53 | 5.421 | 28.5 | .143D+13 | .499D+13 | 3.034 | 28.4 | .107D+13 | .383D+13 | 0.451 | 28.3 | .553D+12 | .202D+13 | 0.045 | 28.4 | .692D+12 | .250D+13 |
| 1.56 | 5.538 | 28.6 | .149D+13 | .815D+13 | 3.089 | 28.5 | .111D+13 | .626D+13 | 0.456 | 28.4 | .567D+12 | .336D+13 | 0.046 | 28.5 | .712D+12 | .413D+13 |
| 1.59 | 5.698 | 28.1 | .158D+13 | .158D+13 | 3.163 | 28.0 | .116D+13 | .116D+13 | 0.463 | 27.9 | .587D+12 | .587D+12 | 0.046 | 28.0 | .739D+12 | .739D+12 |
| 1.66 | 6.070 | 28.9 | .179D+13 | .113D+14 | 3.336 | 28.8 | .129D+13 | .823D+13 | 0.479 | 28.6 | .634D+12 | .381D+13 | 0.048 | 28.7 | .803D+12 | .490D+13 |
| 1.69 | 6.231 | 28.2 | .188D+13 | .299D+13 | 3.409 | 28.1 | .135D+13 | .220D+13 | 0.485 | 28.0 | .654D+12 | .110D+13 | 0.048 | 28.1 | .830D+12 | .138D+13 |
| 1.69 | 6.241 | 28.3 | .189D+13 | .320D+13 | 3.414 | 28.2 | .136D+13 | .233D+13 | 0.486 | 28.1 | .655D+12 | .114D+13 | 0.048 | 28.2 | .832D+12 | .144D+13 |
| 1.75 | 6.562 | 28.4 | .208D+13 | .342D+13 | 3.560 | 28.3 | .148D+13 | .245D+13 | 0.499 | 28.2 | .695D+12 | .115D+13 | 0.049 | 28.3 | .887D+12 | .146D+13 |
| 1.75 | 6.579 | 28.5 | .209D+13 | .718D+13 | 3.568 | 28.4 | .148D+13 | .527D+13 | 0.499 | 28.3 | .697D+12 | .27CD+13 | 0.049 | 28.4 | .890D+12 | .334D+13 |
| 1.76 | 6.601 | 28.9 | .211D+13 | .175D+14 | 3.578 | 28.8 | .149D+13 | .128D+14 | 0.500 | 28.7 | .700D+12 | .634D+13 | 0.049 | 28.7 | .893D+12 | .797D+13 |
| 1.80 | 6.840 | 28.9 | .226D+13 | .166D+14 | 3.685 | 28.8 | .153D+13 | .119D+14 | 0.510 | 28.7 | .729D+12 | .852D+13 | 0.050 | 28.8 | .934D+12 | .707D+13 |
| 1.80 | 6.868 | 29.0 | .227D+13 | .214D+14 | 3.698 | 28.9 | .159D+13 | .151D+14 | 0.511 | 28.8 | .732D+12 | .669D+13 | 0.050 | 28.9 | .939D+12 | .672D+13 |
| 1.81 | 6.896 | 28.6 | .229D+13 | .720D+13 | 3.710 | 28.5 | .160D+13 | .515D+13 | 0.512 | 28.3 | .736D+12 | .246D+13 | 0.050 | 28.4 | .944D+12 | .311D+13 |
| 1.93 | 6.998 | 28.3 | .236D+13 | .390D+13 | 3.756 | 28.2 | .154D+13 | .277D+13 | 0.516 | 28.0 | .748D+12 | .132D+13 | 0.051 | 28.1 | .961D+12 | .167D+13 |
| 1.84 | 7.088 | 28.2 | .242D+13 | .386D+13 | 3.796 | 28.1 | .168D+13 | .274D+13 | 0.519 | 28.0 | .759D+12 | .130D+13 | 0.051 | 28.1 | .976D+12 | .165D+13 |
| 1.86 | 7.202 | 28.4 | .250D+13 | .163D+14 | 3.847 | 28.3 | .172D+13 | .132D+14 | 0.523 | 28.1 | .773D+12 | .113D+15 | 0.051 | 28.2 | .996D+12 | .202D+17 |
| 1.88 | 7.294 | 28.2 | .256D+13 | .414D+13 | 3.888 | 28.1 | .176D+13 | .292D+13 | 0.527 | 27.9 | .784D+12 | .140D+13 | 0.052 | 28.0 | .101D+13 | .176D+13 |
| 1.93 | 7.567 | 28.8 | .275D+13 | .124D+14 | 4.003 | 28.7 | .187D+13 | .865D+13 | 0.537 | 28.5 | .817D+12 | .399D+13 | 0.052 | 28.6 | .106D+13 | .508D+13 |
| 1.96 | 7.732 | 28.6 | .287D+13 | .984D+13 | 4.080 | 28.4 | .194D+13 | .693D+13 | 0.542 | 28.3 | .836D+12 | .352D+13 | 0.053 | 28.4 | .109D+13 | .432D+13 |
| 1.96 | 7.738 | 29.1 | .287D+13 | .227D+14 | 4.082 | 29.0 | .194D+13 | .152D+14 | 0.543 | 28.8 | .837D+12 | .698D+13 | 0.053 | 28.9 | .109D+13 | .801D+13 |
| 1.96 | 7.762 | 28.1 | .239D+13 | .457D+13 | 4.093 | 28.0 | .195D+13 | .319D+13 | 0.544 | 27.9 | .840D+12 | .157D+13 | 0.053 | 28.0 | .109D+13 | .194D+13 |
| 1.98 | 7.892 | 28.0 | .298D+13 | .428D+13 | 4.149 | 27.9 | .200D+13 | .297D+13 | 0.548 | 27.8 | .855D+12 | .146D+13 | 0.053 | 27.9 | .111D+13 | .160D+13 |
| 1.99 | 7.934 | 28.6 | .301D+13 | .600D+13 | 4.168 | 28.5 | .202D+13 | .406D+13 | 0.550 | 28.3 | .860D+12 | .174D+13 | 0.053 | 28.4 | .112D+13 | .226D+13 |
| 2.01 | 8.072 | 29.3 | .312D+13 | .371D+14 | 4.227 | 29.2 | .208D+13 | .243D+14 | 0.554 | 29.0 | .877D+12 | .672D+13 | 0.054 | 29.1 | .114D+13 | .121D+14 |
| 2.06 | 8.388 | 28.3 | .336D+13 | .661D+13 | 4.363 | 28.2 | .221D+13 | .452D+13 | 0.565 | 28.0 | .913D+12 | .218D+13 | 0.055 | 28.1 | .120D+13 | .271D+13 |
| 2.06 | 8.394 | 28.0 | .336D+13 | .425D+13 | 4.366 | 27.9 | .222D+13 | .287D+13 | 0.565 | 27.7 | .914D+12 | .133D+13 | 0.055 | 27.8 | .120D+13 | .167D+13 |
| 2.11 | 8.653 | 28.4 | .357D+13 | .993D+13 | 4.477 | 28.3 | .233D+13 | .691D+13 | 0.574 | 28.1 | .944D+12 | .424D+13 | 0.055 | 28.2 | .124D+13 | .469D+13 |
| 2.12 | 8.722 | 28.6 | .362D+13 | .107D+14 | 4.506 | 28.4 | .236D+13 | .725D+13 | 0.576 | 28.2 | .952D+12 | .357D+13 | 0.056 | 28.3 | .125D+13 | .438D+13 |
| 2.17 | 9.017 | 28.6 | .386D+13 | .112D+14 | 4.631 | 28.5 | .249D+13 | .747D+13 | 0.585 | 28.3 | .986D+12 | .348D+13 | 0.056 | 28.4 | .130D+13 | .435D+13 |
| 2.17 | 9.049 | 29.0 | .389D+13 | .225D+14 | 4.644 | 28.8 | .250D+13 | .147D+14 | 0.586 | 28.6 | .990D+12 | .623D+13 | 0.056 | 28.7 | .131D+13 | .608D+13 |
| 2.33 | 10.08 | 28.3 | .479D+13 | .741D+13 | 5.071 | 28.2 | .298D+13 | .472D+13 | 0.618 | 28.0 | .110D+13 | .197D+13 | 0.059 | 28.1 | .147D+13 | .253D+13 |
| 2.36 | 10.28 | 28.3 | .498D+13 | .693D+13 | 5.153 | 28.1 | .307D+13 | .437D+13 | 0.623 | 27.9 | .113D+13 | .177D+13 | 0.059 | 28.0 | .151D+13 | .229D+13 |
| 2.69 | 12.59 | 28.8 | .739D+13 | .139D+14 | 6.077 | 28.6 | .425D+13 | .804D+13 | 0.685 | 28.3 | .137D+13 | .271D+13 | 0.064 | 28.5 | .187D+13 | .365D+13 |
| 2.83 | 14.03 | 28.5 | .912D+13 | .133D+14 | 6.634 | 28.3 | .504D+13 | .752D+13 | 0.719 | 28.0 | .151D+13 | .26CD+13 | 0.067 | 28.1 | .209D+13 | .343D+13 |

## TABLE 3B

| | (ϵ,e) = (-1.00, -3.50) $\bar{q}_o$=0 | | | | (ϵ,e) = (-0.50, -4.50) $\bar{q}_o$=0 | | | | (ϵ,e) = (0.50, -1.25) $\bar{q}_o$ = 0.50 | | | | (ϵ,e) = (0.92, -1.40) $\bar{q}_o$ = 1.00 | | | |
|---|---|---|---|---|---|---|---|---|---|---|---|---|---|---|---|---|
| Z | $\bar{z}$ | LOG L | V(MPC3) | VM(MPC3) | $\bar{z}$ | LOG L | V(MPC3) | VM(MPC3) | $\bar{z}$ | LOG L | V(MPC3) | VM(MPC3) | $\bar{z}$ | LOG L | V(MPC3) | VM(MPC3) |
| 0.43 | 1.053 | 27.5 | .467D+11 | .302D+12 | 0.715 | 27.5 | .447D+11 | .295D+12 | 0.155 | 27.5 | .378D+11 | .232D+12 | 0.017 | 27.6 | .413D+11 | .248D+12 |
| 0.45 | 1.105 | 27.4 | .521D+11 | .170D+12 | 0.748 | 27.4 | .497D+11 | .163D+12 | 0.161 | 27.4 | .418D+11 | .130D+12 | 0.018 | 27.4 | .457D+11 | .141D+12 |
| 0.49 | 1.209 | 27.6 | .637D+11 | .387D+12 | 0.811 | 27.6 | .603D+11 | .377D+12 | 0.172 | 27.6 | .500D+11 | .294D+12 | 0.019 | 27.6 | .550D+11 | .316D+12 |
| 0.53 | 1.335 | 27.7 | .796D+11 | .667D+12 | 0.889 | 27.7 | .747D+11 | .664D+12 | 0.185 | 27.7 | .608D+11 | .531D+12 | 0.020 | 27.7 | .674D+11 | .561D+12 |
| 0.53 | 1.353 | 27.4 | .820D+11 | .243D+12 | 0.900 | 27.4 | .769D+11 | .232D+12 | 0.187 | 27.4 | .624D+11 | .181D+12 | 0.020 | 27.5 | .693D+11 | .198D+12 |
| 0.54 | 1.365 | 28.1 | .837D+11 | .277D+13 | 0.907 | 28.1 | .784D+11 | .236D+13 | 0.188 | 28.2 | .635D+11 | .256D+13 | 0.021 | 28.2 | .705D+11 | .257D+13 |
| 0.54 | 1.372 | 27.5 | .845D+11 | .248D+12 | 0.911 | 27.5 | .792D+11 | .235D+12 | 0.189 | 27.5 | .640D+11 | .182D+12 | 0.021 | 27.5 | .712D+11 | .200D+12 |
| 0.54 | 1.387 | 28.6 | .866D+11 | .102D+14 | 0.920 | 28.6 | .811D+11 | .104D+14 | 0.190 | 28.7 | .654D+11 | .513D+13 | 0.021 | 28.7 | .728D+11 | .537D+13 |
| 0.55 | 1.415 | 28.2 | .905D+11 | .295D+13 | 0.937 | 28.2 | .846D+11 | .297D+13 | 0.193 | 28.2 | .680D+11 | .238D+13 | 0.021 | 28.3 | .757D+11 | .252D+13 |
| 0.55 | 1.419 | 28.0 | .909D+11 | .935D+12 | 0.939 | 28.0 | .850D+11 | .898D+12 | 0.193 | 28.0 | .683D+11 | .657D+12 | 0.021 | 28.0 | .760D+11 | .724D+12 |
| 0.56 | 1.424 | 28.1 | .918D+11 | .169D+13 | 0.943 | 28.1 | .858D+11 | .166D+13 | 0.194 | 28.1 | .688D+11 | .125D+13 | 0.021 | 28.1 | .767D+11 | .135D+13 |
| 0.56 | 1.437 | 27.7 | .936D+11 | .568D+12 | 0.950 | 27.7 | .873D+11 | .546D+12 | 0.195 | 27.8 | .700D+11 | .411D+12 | 0.021 | 27.8 | .780D+11 | .451D+12 |
| 0.57 | 1.468 | 28.0 | .981D+11 | .174D+13 | 0.969 | 28.0 | .914D+11 | .177D+13 | 0.198 | 28.0 | .729D+11 | .150D+13 | 0.022 | 28.0 | .814D+11 | .154D+13 |
| 0.57 | 1.477 | 27.9 | .995D+11 | .180D+13 | 0.975 | 27.9 | .926D+11 | .188D+13 | 0.199 | 27.9 | .738D+11 | .181D+13 | 0.022 | 28.0 | .824D+11 | .175D+13 |
| 0.60 | 1.544 | 27.8 | .110D+12 | .154D+13 | 1.014 | 27.8 | .102D+12 | .160D+13 | 0.205 | 27.9 | .801D+11 | .151D+13 | 0.022 | 27.9 | .898D+11 | .147D+13 |
| 0.60 | 1.557 | 27.7 | .112D+12 | .471D+12 | 1.022 | 27.7 | .103D+12 | .445D+12 | 0.207 | 27.7 | .814D+11 | .331D+12 | 0.023 | 27.8 | .912D+11 | .368D+12 |
| 0.61 | 1.605 | 27.9 | .119D+12 | .899D+12 | 1.050 | 27.9 | .110D+12 | .857D+12 | 0.211 | 27.9 | .861D+11 | .627D+12 | 0.023 | 28.0 | .967D+11 | .695D+12 |
| 0.61 | 1.605 | 27.8 | .119D+12 | .628D+12 | 1.050 | 27.8 | .110D+12 | .595D+12 | 0.211 | 27.8 | .861D+11 | .438D+12 | 0.023 | 27.9 | .967D+11 | .487D+12 |
| 0.62 | 1.611 | 28.1 | .120D+12 | .161D+13 | 1.054 | 28.1 | .111D+12 | .156D+13 | 0.212 | 28.1 | .867D+11 | .116D+13 | 0.023 | 28.1 | .975D+11 | .127D+13 |
| 0.63 | 1.641 | 28.3 | .125D+12 | .303D+13 | 1.071 | 28.3 | .115D+12 | .292D+13 | 0.214 | 28.3 | .896D+11 | .209D+13 | 0.023 | 28.4 | .101D+12 | .232D+13 |
| 0.63 | 1.657 | 27.6 | .128D+12 | .336D+12 | 1.081 | 27.6 | .117D+12 | .314D+12 | 0.216 | 27.6 | .912D+11 | .235D+12 | 0.023 | 27.6 | .103D+12 | .262D+12 |
| 0.64 | 1.693 | 28.1 | .134D+12 | .988D+12 | 1.102 | 28.1 | .123D+12 | .922D+12 | 0.219 | 28.1 | .949D+11 | .643D+12 | 0.024 | 28.1 | .107D+12 | .727D+12 |
| 0.65 | 1.729 | 28.2 | .140D+12 | .205D+13 | 1.123 | 28.2 | .128D+12 | .199D+13 | 0.222 | 28.2 | .986D+11 | .147D+13 | 0.024 | 28.2 | .111D+12 | .161D+13 |
| 0.66 | 1.752 | 27.6 | .144D+12 | .353D+12 | 1.137 | 27.6 | .132D+12 | .328D+12 | 0.224 | 27.6 | .101D+12 | .244D+12 | 0.024 | 27.6 | .114D+12 | .273D+12 |
| 0.67 | 1.786 | 28.1 | .150D+12 | .194D+13 | 1.156 | 28.1 | .137D+12 | .147D+13 | 0.227 | 28.1 | .104D+12 | .108D+13 | 0.025 | 28.1 | .118D+12 | .119D+13 |
| 0.67 | 1.796 | 27.8 | .152D+12 | .128D+13 | 1.162 | 27.8 | .138D+12 | .128D+13 | 0.228 | 27.8 | .105D+12 | .106D+13 | 0.025 | 27.9 | .120D+12 | .113D+13 |
| 0.68 | 1.812 | 27.4 | .155D+12 | .249D+12 | 1.172 | 27.4 | .141D+12 | .229D+12 | 0.230 | 27.4 | .107D+12 | .172D+12 | 0.025 | 27.5 | .122D+12 | .193D+12 |
| 0.68 | 1.836 | 28.0 | .159D+12 | .367D+13 | 1.186 | 28.0 | .145D+12 | .418D+13 | 0.232 | 28.0 | .110D+12 | .113D+15 | 0.025 | 28.0 | .125D+12 | .820D+13 |
| 0.68 | 1.836 | 27.5 | .159D+12 | .311D+12 | 1.185 | 27.5 | .145D+12 | .287D+12 | 0.232 | 27.5 | .110D+12 | .213D+12 | 0.025 | 27.6 | .125D+12 | .240D+12 |
| 0.69 | 1.863 | 28.8 | .164D+12 | .329D+14 | 1.201 | 28.8 | .149D+12 | .376D+14 | 0.234 | 28.8 | .113D+12 | .113D+16 | 0.025 | 28.8 | .128D+12 | .202D+17 |
| 0.70 | 1.887 | 27.7 | .168D+12 | .839D+12 | 1.215 | 27.7 | .153D+12 | .812D+12 | 0.236 | 27.7 | .115D+12 | .633D+12 | 0.025 | 27.7 | .131D+12 | .685D+12 |
| 0.72 | 1.958 | 27.7 | .182D+12 | .890D+12 | 1.256 | 27.7 | .165D+12 | .860D+12 | 0.242 | 27.7 | .123D+12 | .674D+12 | 0.026 | 27.7 | .140D+12 | .728D+12 |
| 0.72 | 1.958 | 27.9 | .182D+12 | .155D+13 | 1.256 | 27.9 | .165D+12 | .155D+13 | 0.242 | 27.9 | .123D+12 | .133D+13 | 0.026 | 27.9 | .140D+12 | .138D+13 |
| 0.73 | 1.989 | 27.4 | .188D+12 | .346D+12 | 1.273 | 27.4 | .170D+12 | .320D+12 | 0.245 | 27.4 | .126D+12 | .240D+12 | 0.026 | 27.4 | .144D+12 | .268D+12 |
| 0.73 | 1.996 | 27.5 | .190D+12 | .280D+12 | 1.277 | 27.5 | .171D+12 | .254D+12 | 0.245 | 27.5 | .127D+12 | .186D+12 | 0.026 | 27.6 | .145D+12 | .212D+12 |
| 0.73 | 2.007 | 28.5 | .192D+12 | .420D+13 | 1.283 | 28.5 | .173D+12 | .392D+13 | 0.246 | 28.5 | .128D+12 | .259D+13 | 0.026 | 28.5 | .146D+12 | .298D+13 |
| 0.76 | 2.098 | 28.3 | .211D+12 | .624D+13 | 1.335 | 28.3 | .189D+12 | .646D+13 | 0.254 | 28.3 | .138D+12 | .939D+13 | 0.027 | 28.4 | .159D+12 | .725D+13 |
| 0.76 | 2.115 | 28.0 | .214D+12 | .990D+12 | 1.345 | 27.9 | .192D+12 | .913D+12 | 0.255 | 27.9 | .140D+12 | .640D+12 | 0.027 | 28.0 | .161D+12 | .726D+12 |
| 0.77 | 2.126 | 28.4 | .217D+12 | .352D+13 | 1.351 | 28.4 | .194D+12 | .326D+13 | 0.256 | 28.4 | .141D+12 | .216D+13 | 0.027 | 28.5 | .162D+12 | .249D+13 |
| 0.79 | 2.204 | 27.6 | .234D+12 | .355D+12 | 1.395 | 27.6 | .208D+12 | .319D+12 | 0.262 | 27.6 | .150D+12 | .226D+12 | 0.028 | 27.7 | .173D+12 | .260D+12 |
| 0.83 | 2.342 | 27.5 | .265D+12 | .351D+12 | 1.472 | 27.5 | .234D+12 | .312D+12 | 0.273 | 27.5 | .166D+12 | .221D+12 | 0.029 | 27.5 | .192D+12 | .254D+12 |
| 0.85 | 2.419 | 28.4 | .284D+12 | .157D+14 | 1.514 | 28.4 | .249D+12 | .179D+14 | 0.279 | 28.4 | .175D+12 | .113D+15 | 0.030 | 28.5 | .203D+12 | .202D+17 |
| 0.85 | 2.430 | 27.8 | .286D+12 | .105D+13 | 1.520 | 27.7 | .251D+12 | .983D+12 | 0.280 | 27.7 | .176D+12 | .737D+12 | 0.030 | 27.8 | .205D+12 | .814D+12 |
| 0.86 | 2.456 | 29.2 | .293D+12 | .599D+13 | 1.535 | 28.2 | .256D+12 | .637D+13 | 0.281 | 28.1 | .179D+12 | .113D+15 | 0.030 | 28.2 | .209D+12 | .110D+14 |
| 0.86 | 2.463 | 27.7 | .294D+12 | .823D+12 | 1.539 | 27.7 | .258D+12 | .762D+12 | 0.282 | 27.7 | .180D+12 | .883D+12 | 0.030 | 27.7 | .210D+12 | .621D+12 |
| 0.87 | 2.501 | 28.1 | .304D+12 | .183D+13 | 1.559 | 28.1 | .265D+12 | .167D+13 | 0.285 | 28.1 | .185D+12 | .115D+13 | 0.030 | 28.1 | .215D+12 | .131D+13 |
| 0.87 | 2.501 | 27.5 | .304D+12 | .612D+12 | 1.559 | 27.5 | .265D+12 | .556D+12 | 0.285 | 27.5 | .185D+12 | .407D+12 | 0.030 | 27.6 | .215D+12 | .453D+12 |
| 0.87 | 2.504 | 29.1 | .305D+12 | .391D+14 | 1.561 | 29.1 | .266D+12 | .275D+14 | 0.285 | 29.0 | .185D+12 | .178D+14 | 0.030 | 29.1 | .216D+12 | .214D+14 |
| 0.88 | 2.516 | 28.1 | .307D+12 | .135D+13 | 1.567 | 28.0 | .268D+12 | .121D+13 | 0.286 | 28.0 | .186D+12 | .815D+12 | 0.030 | 28.1 | .217D+12 | .540D+12 |
| 0.89 | 2.572 | 27.9 | .322D+12 | .995D+12 | 1.598 | 27.9 | .280D+12 | .896D+12 | 0.290 | 27.8 | .193D+12 | .615D+12 | 0.031 | 27.9 | .225D+12 | .706D+12 |
| 0.90 | 2.591 | 28.1 | .327D+12 | .140D+13 | 1.609 | 28.0 | .284D+12 | .125D+13 | 0.291 | 28.0 | .195D+12 | .839D+12 | 0.031 | 28.1 | .228D+12 | .969D+12 |
| 0.90 | 2.614 | 27.6 | .333D+12 | .574D+12 | 1.621 | 27.6 | .289D+12 | .510D+12 | 0.293 | 27.5 | .198D+12 | .354D+12 | 0.031 | 27.6 | .232D+12 | .408D+12 |
| 0.90 | 2.625 | 28.5 | .336D+12 | .120D+14 | 1.627 | 28.5 | .291D+12 | .120D+14 | 0.294 | 28.5 | .200D+12 | .113D+15 | 0.031 | 28.6 | .233D+12 | .147D+14 |
| 0.91 | 2.633 | 28.2 | .338D+12 | .275D+13 | 1.631 | 28.2 | .293D+12 | .254D+13 | 0.294 | 28.2 | .200D+12 | .180D+13 | 0.031 | 28.2 | .234D+12 | .203D+13 |
| 0.91 | 2.663 | 28.2 | .346D+12 | .276D+13 | 1.648 | 28.1 | .299D+12 | .257D+13 | 0.297 | 28.1 | .204D+12 | .191D+13 | 0.031 | 28.2 | .239D+12 | .211D+13 |
| 0.93 | 2.713 | 28.4 | .359D+12 | .398D+13 | 1.675 | 28.4 | .310D+12 | .358D+13 | 0.300 | 28.4 | .210D+12 | .233D+13 | 0.032 | 28.4 | .246D+12 | .271D+13 |
| 0.94 | 2.764 | 28.5 | .373D+12 | .751D+13 | 1.702 | 28.5 | .321D+12 | .696D+13 | 0.304 | 28.5 | .216D+12 | .525D+13 | 0.032 | 28.6 | .254D+12 | .880D+13 |
| 0.96 | 2.846 | 28.3 | .396D+12 | .247D+13 | 1.746 | 28.3 | .339D+12 | .218D+13 | 0.309 | 28.3 | .226D+12 | .138D+13 | 0.032 | 28.3 | .266D+12 | .162D+13 |
| 0.96 | 2.849 | 28.6 | .397D+12 | .528D+13 | 1.748 | 28.5 | .339D+12 | .465D+13 | 0.309 | 28.5 | .227D+12 | .285D+13 | 0.033 | 28.6 | .267D+12 | .339D+13 |
| 0.98 | 2.920 | 28.3 | .417D+12 | .370D+13 | 1.786 | 28.2 | .355D+12 | .340D+13 | 0.314 | 28.2 | .236D+12 | .254D+13 | 0.033 | 28.3 | .278D+12 | .281D+13 |
| 1.01 | 3.048 | 28.2 | .455D+12 | .233D+13 | 1.854 | 28.2 | .385D+12 | .206D+13 | 0.323 | 28.1 | .251D+12 | .135D+13 | 0.034 | 28.2 | .298D+12 | .157D+13 |

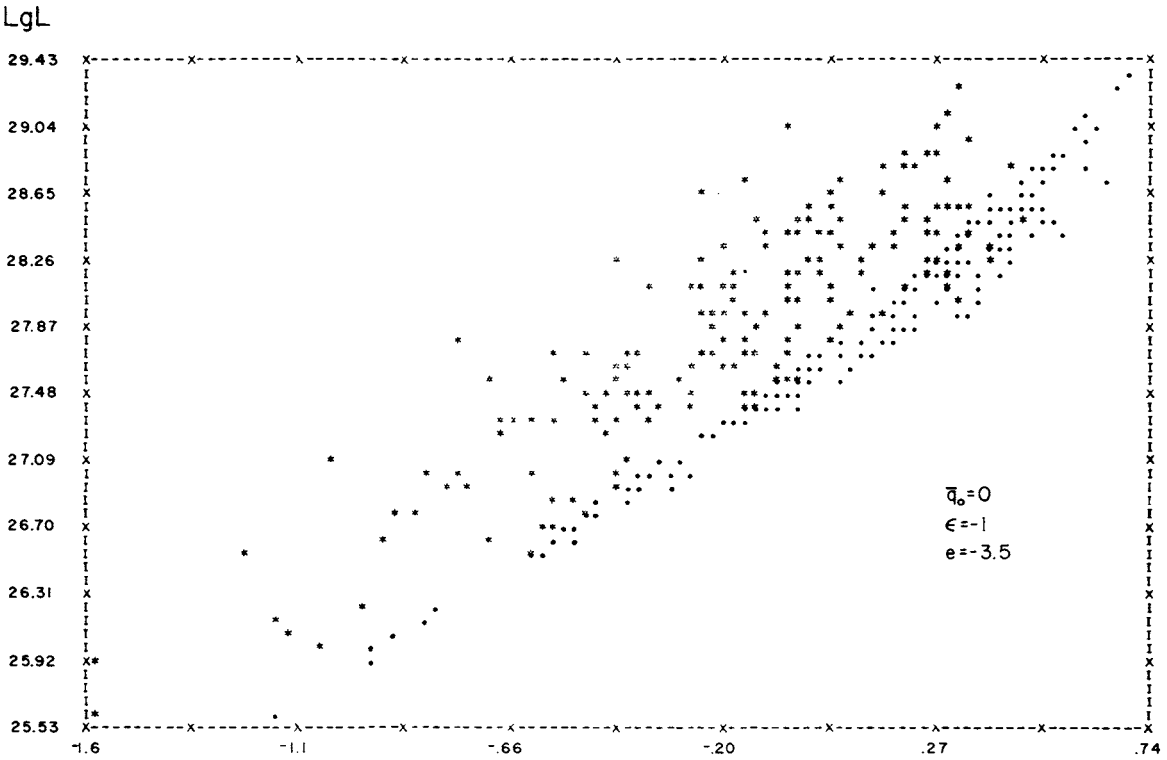


FIG. 2a

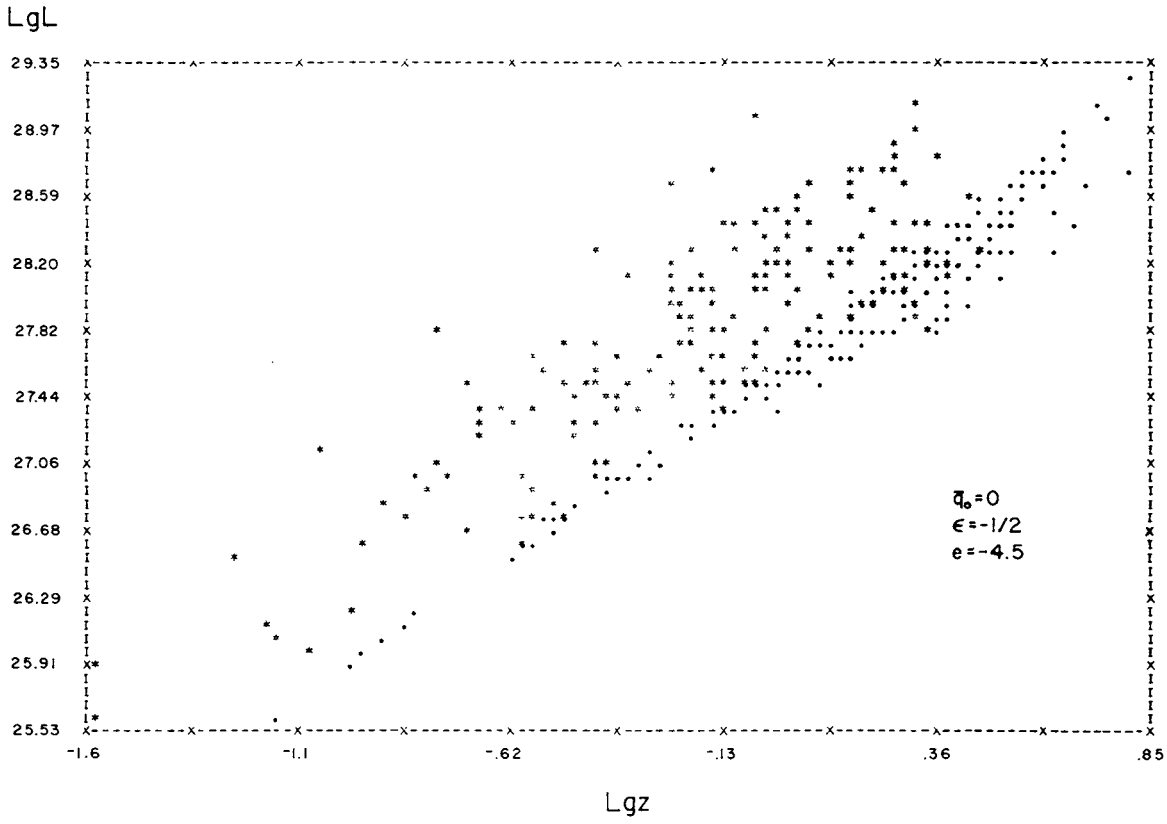


FIG. 2b

FIGS. 2a–2d.—$\mathrm{Log}_{10} L$ (W $\mathrm{Hz}^{-1}$) versus observed $z$ (*asterisks*) and $z_M$ (*dots*) from our data, corresponding to selected cases from Fig. 3, detailed in Table 3.

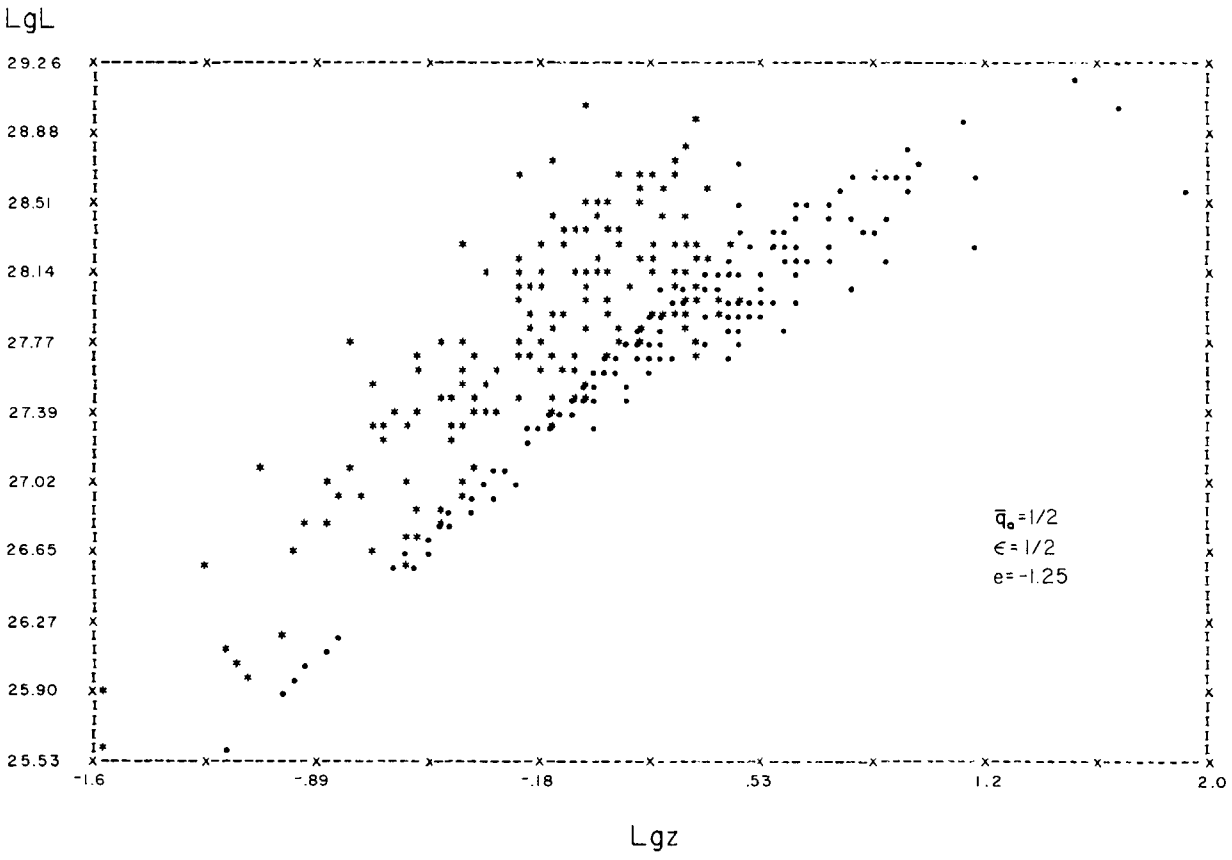


FIG. 2c

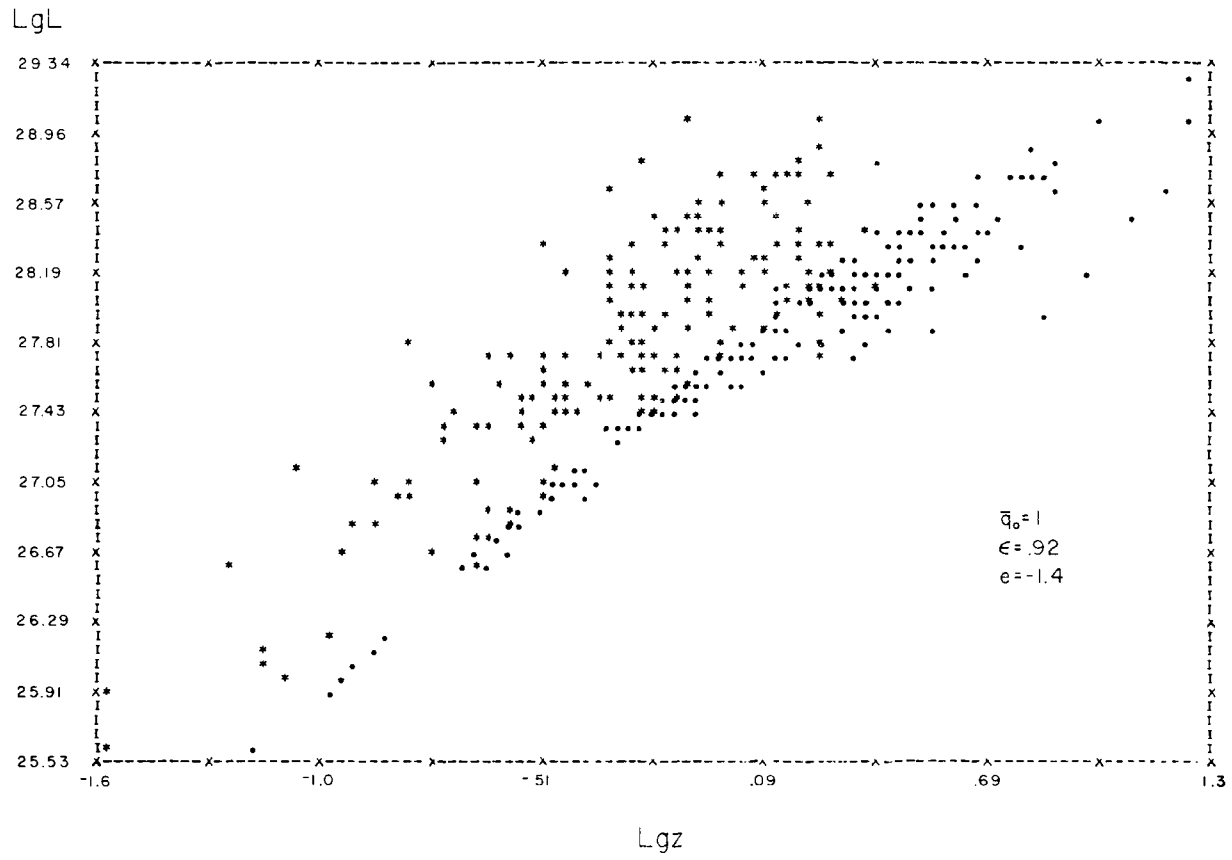


FIG. 2d

which, since $dt$ and $R(t)$ scale the same way, holds true in gravitational units, i.e.,

$$d\chi = \frac{cd\bar{t}}{\bar{R}(\bar{t})} . \tag{6.3b}$$

Just as in standard cosmology, this metric leads to

$$V(t_0, \chi) = 4\pi R_0^3 \int_0^{\chi} \Sigma^2(\chi') d\chi' , \tag{6.4}$$

with the limit given by

$$\chi = c \int_{\bar{t}_e}^{\bar{t}_0} \frac{d\bar{t}}{\bar{R}(\bar{t})} , \tag{6.5}$$

where the limits $\bar{t}_0$ and $\bar{t}_e$ correspond to $\varkappa = 0$ and $\varkappa$, which in turn corresponds to the emission redshift $z$ in atomic units as in equation (3.4).

The values $z$, $\varkappa$, $L$ (watt-sec), $V(\mathrm{Mpc}^3)$, and $V_{\max}(\mathrm{Mpc}^3)$ are given in Table 3.

Once the luminosities and maximum observable volumes are obtained, plots of $\log L$ versus $\log z$ and $\log L$ versus $\log z_M$ are made. Examples are given in Figures 2. The $\log L$ axis is divided into overlapping one unit intervals, one-half unit apart, and the smallest $z_M = z_{MS}$ (corresponding to the weakest source in the interval when one spectral index is used as $\alpha = -0.8$ in Petrosian 1969) is found among the sources in each interval. The number of sources in the interval whose $z < z_{MS}$ is counted. This number is divided by the volume corresponding to $z_{MS}$ to give $\varphi$ for each $L$ interval, and a best fit of $\ln \varphi = \ln C - n \ln L$ is made in order to find $n$. The second method of obtaining the RLF, which we denote by an asterisk $\varphi^*(L)$ in order to differentiate it from the first one, is to sum up all the reciprocal volumes corresponding to the $z_M$ in each interval and make the same power law approximation, $\log \varphi^* = \log C^* - n^* \log L$. We found that $n^*$ determined this way differed very little from $n$ determined by the first method, $n^*$ being generally slightly smaller than $n$.

In Table 4 we present the values of $n$ that we have determined as a function of $\epsilon$, $\bar{q}_0$, and $e$. As seen from the table, the values of $n$ cover quite a range from 0.2 to 2.4 depending on the chosen gauge and evolution. In Figures 3*a*–3*c* we then present three typical RLF's for $\bar{q}_0 = 0, +\frac{1}{2}$, and 1. We note that the RLF steepens as $L$ increases

TABLE 4

EXPONENT $n$ OF RLF (eq. [4.5]) FOR $\alpha = -0.75$

| $\epsilon$ | $e/\bar{q}_0$ | 0 | $\frac{1}{2}$ | 1 |
|---|---|---|---|---|
| −1..... | −4.50 | 1.55 | ... | ... |
| | −4.00 | ... | ... | 1.35 |
| | −3.50 | 1.11 | 1.46 | ... |
| | −1.58 | 0.879 | 0.759 | ... |
| | −1.50 | 0.876 | 0.734 | 0.399 |
| | −1.45 | 0.861 | 0.726 | ... |
| | −1.25 | 0.822 | 0.728 | 0.270 |
| | 0.00 | 0.735 | 0.489 | 0.257 |
| | +2.00 | 0.640 | 0.305 | 0.192 |
| $-\frac{1}{2}$..... | −8.00 | 2.04 | 1.91 | ... |
| | −5.00 | 1.21 | 1.02 | ... |
| | −4.50 | 1.14 | 1.12 | ... |
| | −4.00 | 1.04 | ... | ... |
| | −1.65 | 0.879 | 0.886 | ... |
| | −0.80 | 0.897 | 0.776 | 0.774 |
| | 0.00 | 0.825 | 0.755 | 0.695 |
| | +2.00 | 0.754 | 0.553 | 0.515 |
| $+\frac{1}{2}$..... | −2.00 | ... | 0.956 | 0.959 |
| | −1.25 | 0.957 | 1.11 | 1.17 |
| | −1.00 | 0.988 | 1.15 | ... |
| | −0.50 | 1.07 | ... | 1.44 |
| | 0.00 | 1.22 | 1.38 | ... |
| | +1.00 | 1.58 | 1.79 | ... |
| +0.92 ... | −2.00 | 1.03 | 1.03 | 1.03 |
| | −1.40 | 1.05 | 1.05 | 1.05 |
| | −1.20 | 1.07 | 1.07 | 1.07 |
| | −1.20 | 1.08 | 1.09 | ... |
| | −0.50 | ... | ... | 2.08 |
| | 0.00 | 2.41 | 2.34 | ... |

NOTE.—Three digits are retained for easy reading but are obviously not significant.

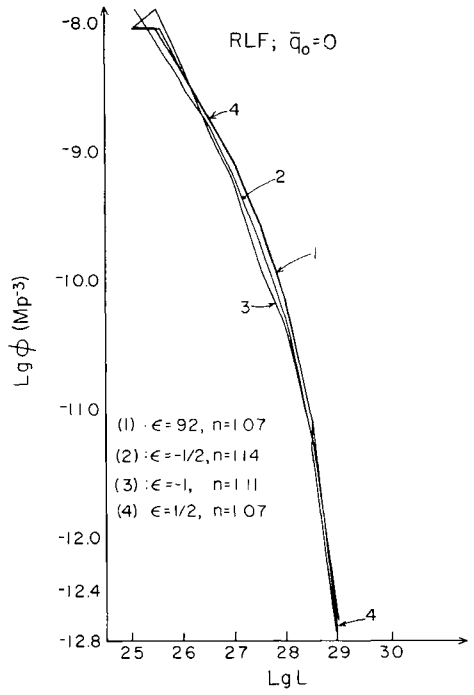


FIG. 3a

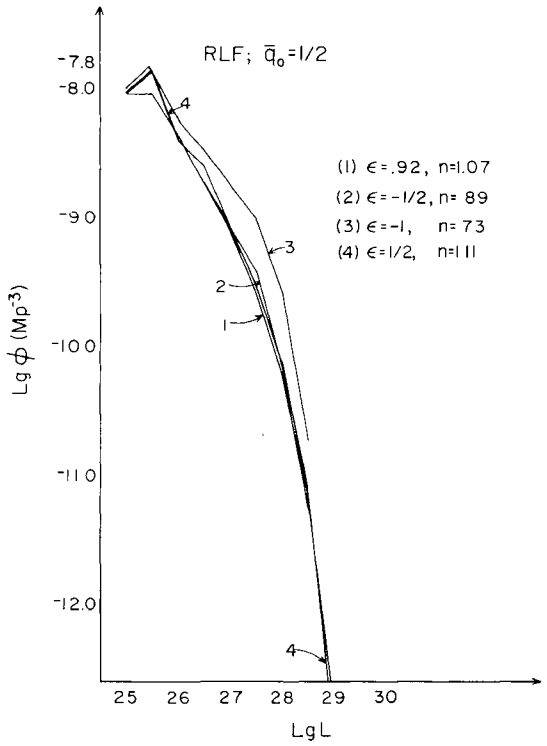


FIG. 3b

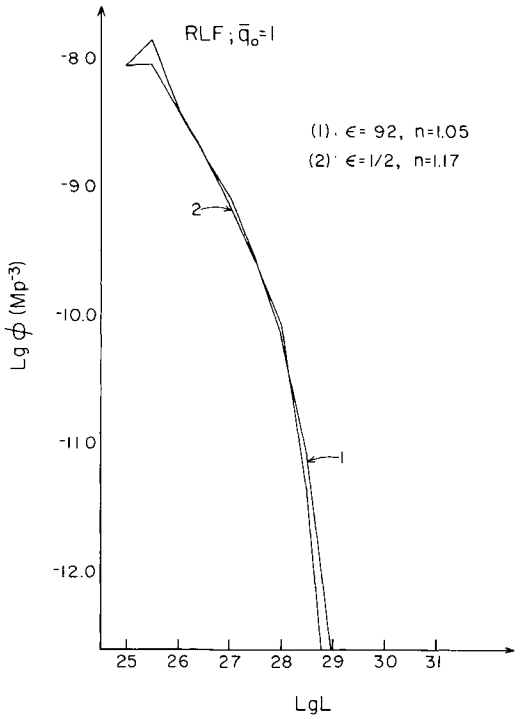


FIG. 3c

FIG. 3.—The RLF corresponding to Table 5, some cases of which are further illustrated in Figures 2*a*–2*d* and Table 2. They correspond to the following evolutionary parameters: Fig. 3*a*.—(1) $e = -1.28$, (2) $e = -4.5$, (3) $e = -3.5$, (4) $e = -0.5$. Fig. 3*b*.—(1) $e = -1.28$, (2) $e = -1.65$, (3) $e = -1.45$, (4) $e = -1.25$. Fig. 3*c*.—(1) $e = -1.40$, (2) $b = -1.25$. The RLF for $\bar{q}_0 = 1$, $\epsilon < 0$, is not presented because the corresponding calculated log $N$–log $S$ curve did not fit the data well.

and a power law is certainly only a first approximation just as in standard cosmology. We have chosen to present cases compatible with the data, and this is partly responsible for the coincidence of the RLFs for different scales.

We reran our program with data compiled by Soltan (1978*a*, *b*) with criteria of completeness. His sample contains fewer high-$z$ sources, and has a higher $n$ and thus a flatter $N(S)$ curve for the same $\epsilon$, $\bar{q}_0$, $e$. Nevertheless, the general conclusions of the paper are the same, even less evolution being required for the same results when $\epsilon < 0$.

## VII. RESULTS

Using the values of the spectral index $n$ so obtained, we have computed numerically the differential counts as from (4.6).

In Figures 4*a*–4*j* we present the results for 30 selected cases, for the four gauges $\epsilon = -1, -\frac{1}{2}, +\frac{1}{2}, 0.92$. For the first three gauges, we present the results for $\bar{q}_0 = 0, \frac{1}{2}$, and 1. For the last gauge, we present only the results for $\bar{q}_0 = 0$ since, as seen from Table 4, the values of $n$ are very insensitive to changes in $\bar{q}_0$. The theoretical curves are superposed on the same data used by von Hoerner (1973). We have fixed the normalization to be $n_n(1\ \mathrm{Jy}) = 1$.

The following comments are in order upon inspecting the results.

1. When $\epsilon$ is negative, the results depend sensitively on $\bar{q}_0$. When $\epsilon$ is positive, they do not. This same feature characterizes the tests studied in Paper III.
2. It follows that for $\epsilon < 0$, there is a clear deterioration of the fits as $\bar{q}_0$ increases.
3. For $\epsilon < 0$, a closed universe model does not fit the data.
4. For $\epsilon > 0$, the data can be fitted with a closed or open universe (see also Paper III).
5. For each of the cases presented in Figures 4*a*–4*j*, we have selected the best fits and summarized the characteristic parameters in Table 5.
6. In the same table we have also added a column giving the value of $E$, the evolutionary parameter as defined in standard cosmology, equations (2.14) and (2.15).
7. Such values of $E$ are obtainable as a function of $e$, $\epsilon$, and $\bar{q}_0$ using (3.4) and (5.2). In the case of $\bar{q}_0 = 0$ or $\frac{1}{2}$, the relation is exact, whereas for other values of $\bar{q}_0$ it is approximate.

We deduce

$$E = \frac{e\epsilon}{H_0 t_0} \cdot \tag{7.1}$$

The ratio $E/e$ is also given in column (D) of Table 1, and the value of $e$ which corresponds to $E = 5$ is given in column (E) of the same table.

## VIII. DISCUSSION

Two major conclusions follow from our analysis. A self-consistent treatment of the parameters entering the problem, especially $n$, yields results that fit the data very satisfactorily, even when the "gravitational constant" $G$ varies with time as $t^{-1}$.

When $\epsilon > 0$, the results are not very different from those of standard cosmology, whereas for $\epsilon < 0$ it is possible to discriminate between an open and a closed universe. This does not happen in standard cosmology. Evolution of the sources is needed as in standard cosmology. In fact, the main effect of our cosmology is the disentanglement of atomic from gravitational times, not the determination of a parameter like $E$ or $e$ which depends on the physics of the problem and only marginally on cosmology.

TABLE 5

EVOLUTIONARY PARAMETER $e$ (eq. [2.15]) YIELDING BEST FIT OF DIFFERENTIAL LOG $N$–LOG $S$ DATA ($\alpha = -0.75$)

| $\bar{q}_0$ | $\epsilon$ | $e$ | $n$ | $E$ | $p$ |
|---|---|---|---|---|---|
| 0..... | −1.00 | −3.50 | 1.110 | +3.50 | −1.1875 |
| | −0.50 | −4.50 | 1.140 | +2.25 | −1.1667 |
| | +0.50 | −0.50 | 1.070 | −0.25 | −1.0000 |
| | +0.92 | −1.28 | 1.070 | −1.18 | −0.4525 |
| ½..... | −1.00 | −1.45 | 0.726 | +4.35 | −0.9500 |
| | −0.50 | −1.65 | 0.886 | +1.65 | −0.9750 |
| | +0.50 | −1.25 | 1.110 | −1.75 | −0.8750 |
| | +0.92 | −1.28 | 1.070 | −1.21 | −0.6988 |
| 1..... | +0.50 | −1.25 | 1.170 | −0.80 | −1.0010 |
| | +0.92 | −1.40 | 1.050 | −1.33 | +0.5101 |

NOTE.—For each $\epsilon$, $q_0$ investigated, with $\alpha = -0.75$, we present the $e$ which gave the best fit to the differential $N(S)$ data with the corresponding $n$, equivalent $E$ as defined by eq. (5.11), and $p$ as given by eq. (3.7).

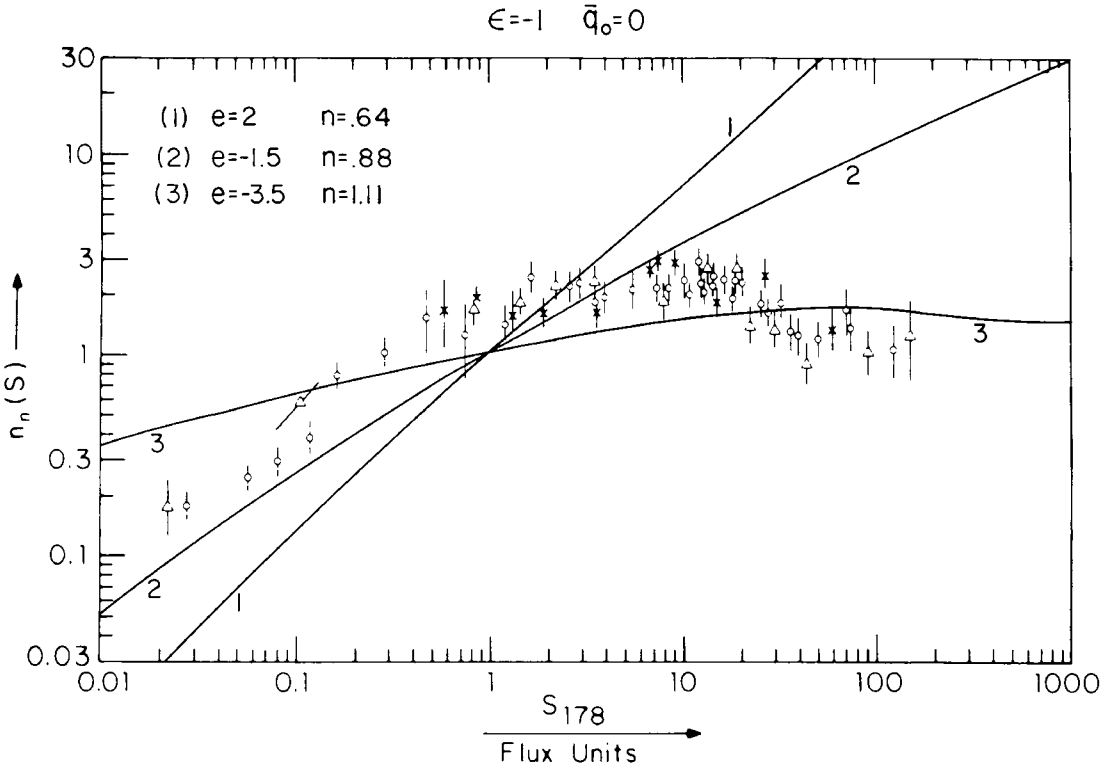


FIG. 4a

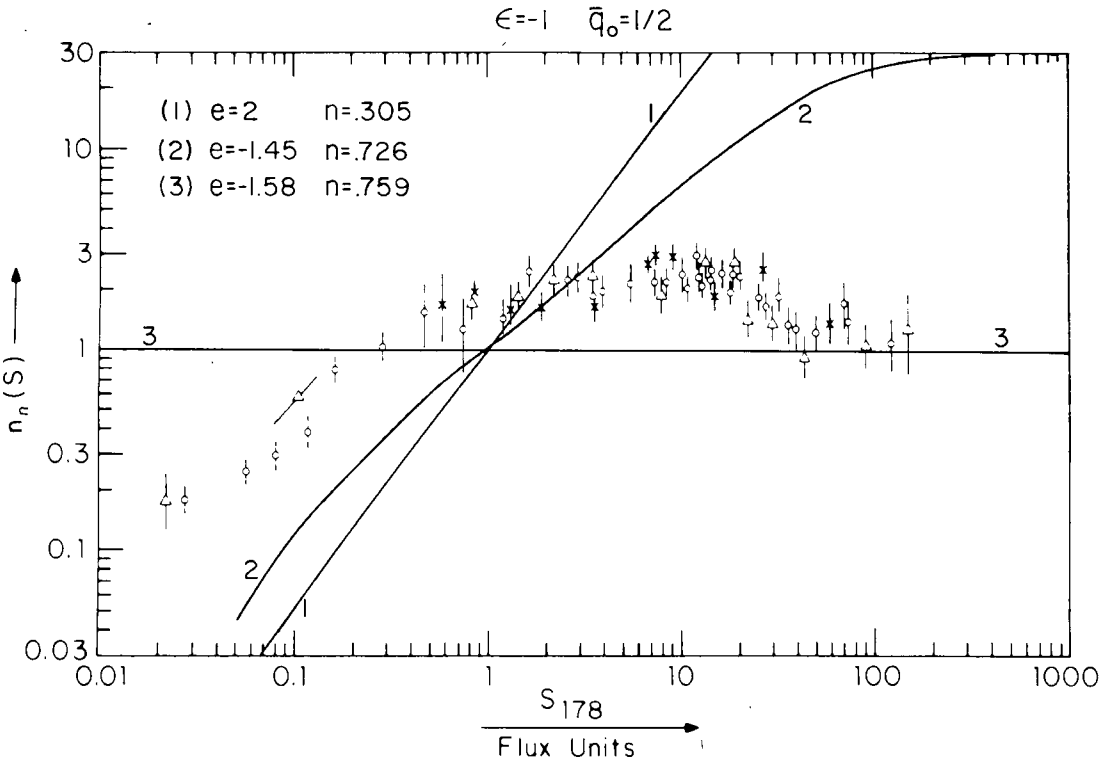


FIG. 4b

FIGS. 4*a*–4*j*.—Log–log plots of eq. (5.1), $N(S)$, the differential radio source counts normalized to Euclidean values. All curves are made to pass through the point $(N, S) = (1, 1)$. Such vertical normalization is customary.

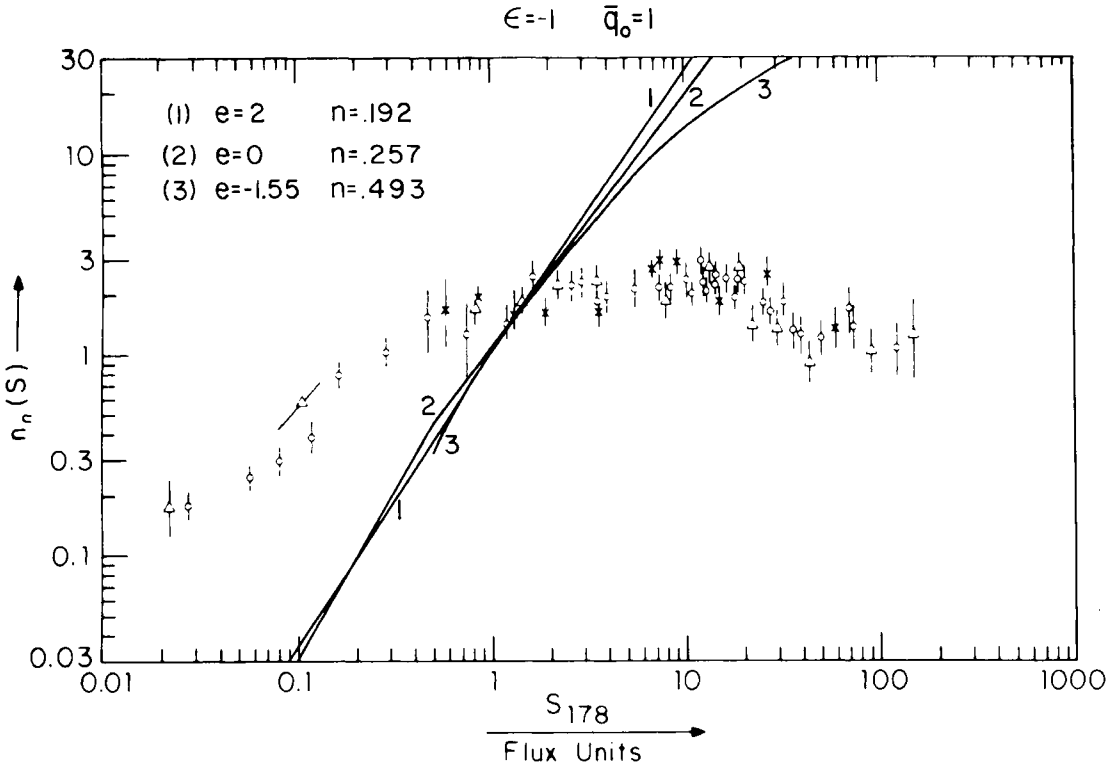


FIG. 4c

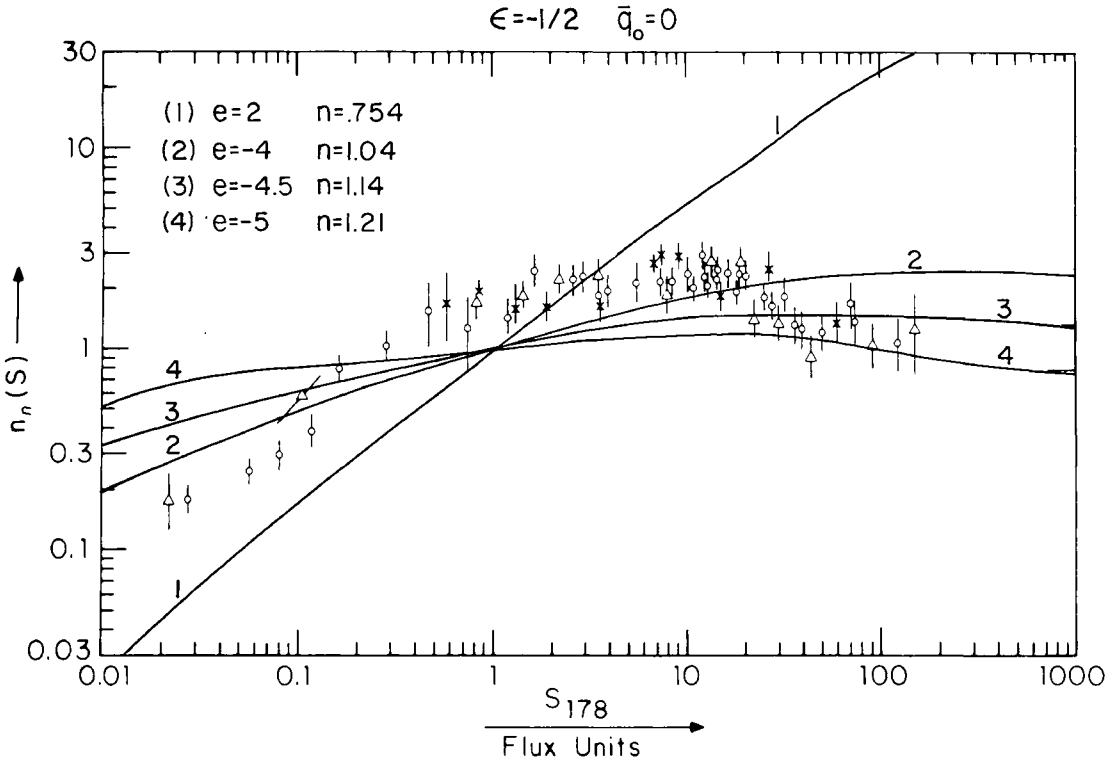


FIG. 4d

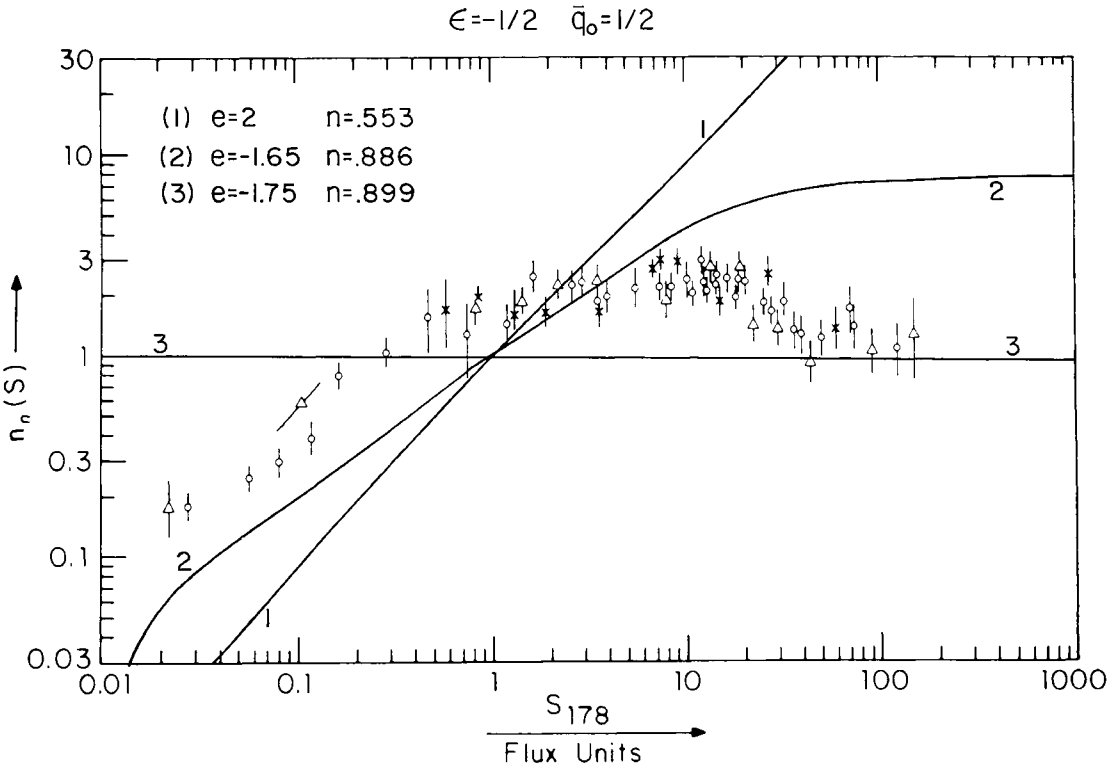


FIG. 4e

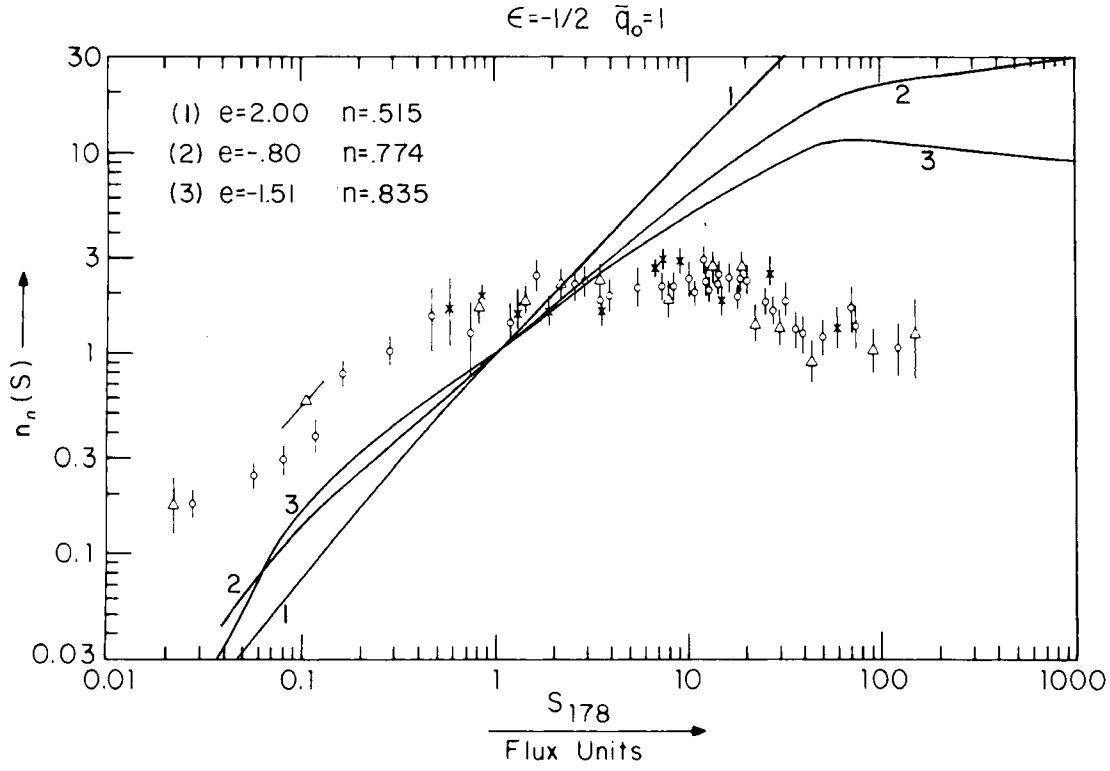


FIG. 4f

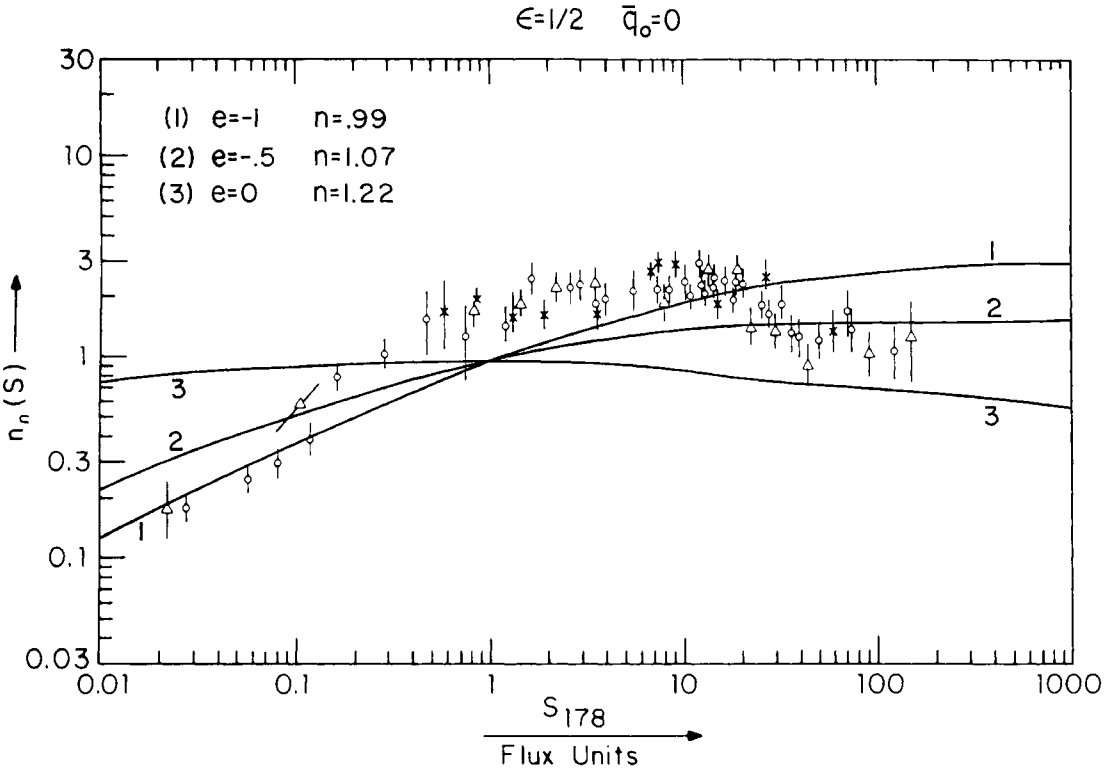


FIG. 4g

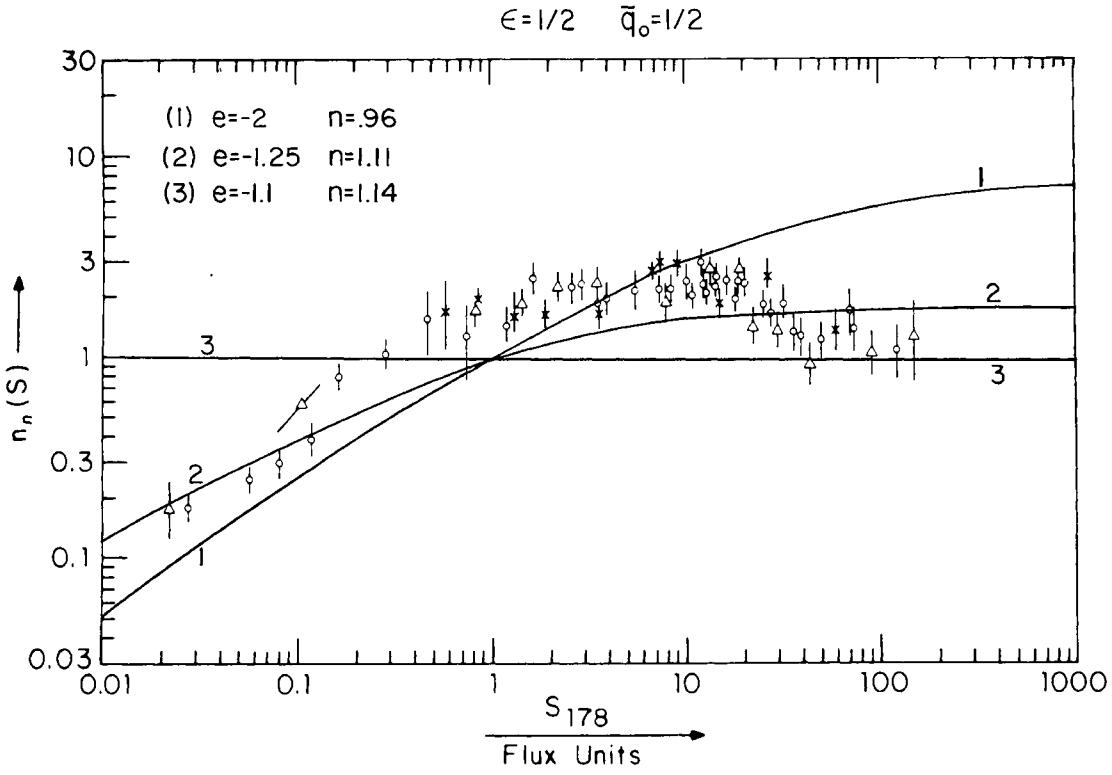


FIG. 4h

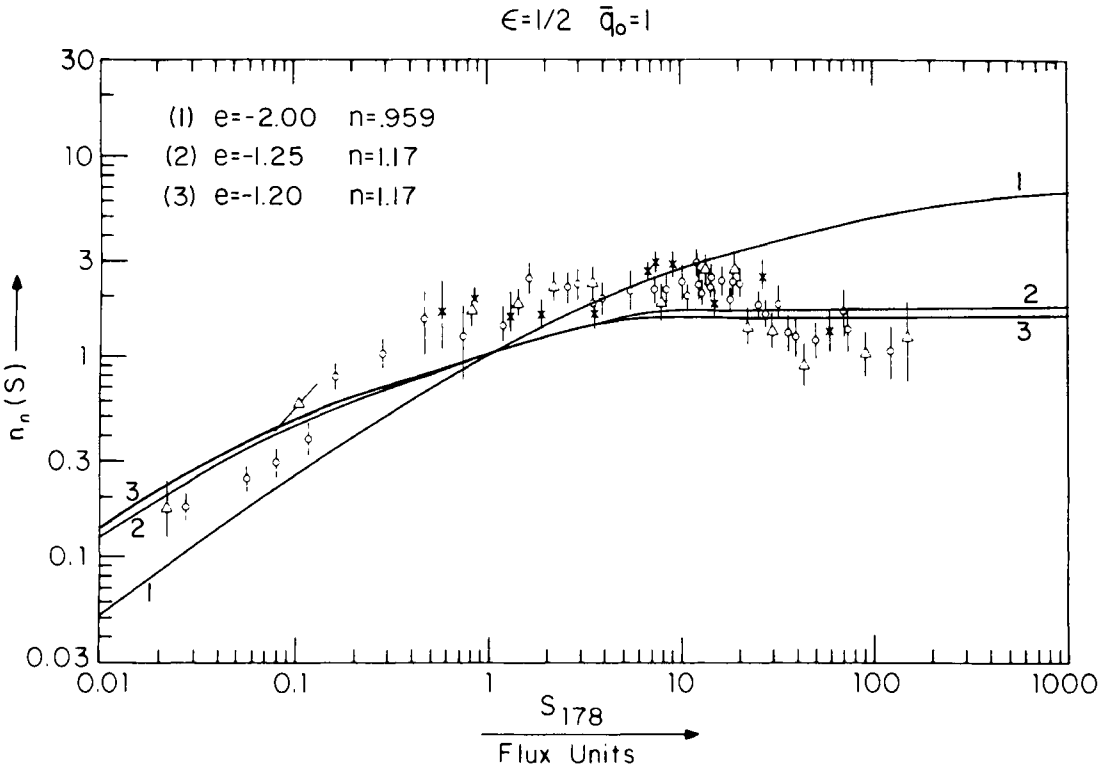


FIG. 4i

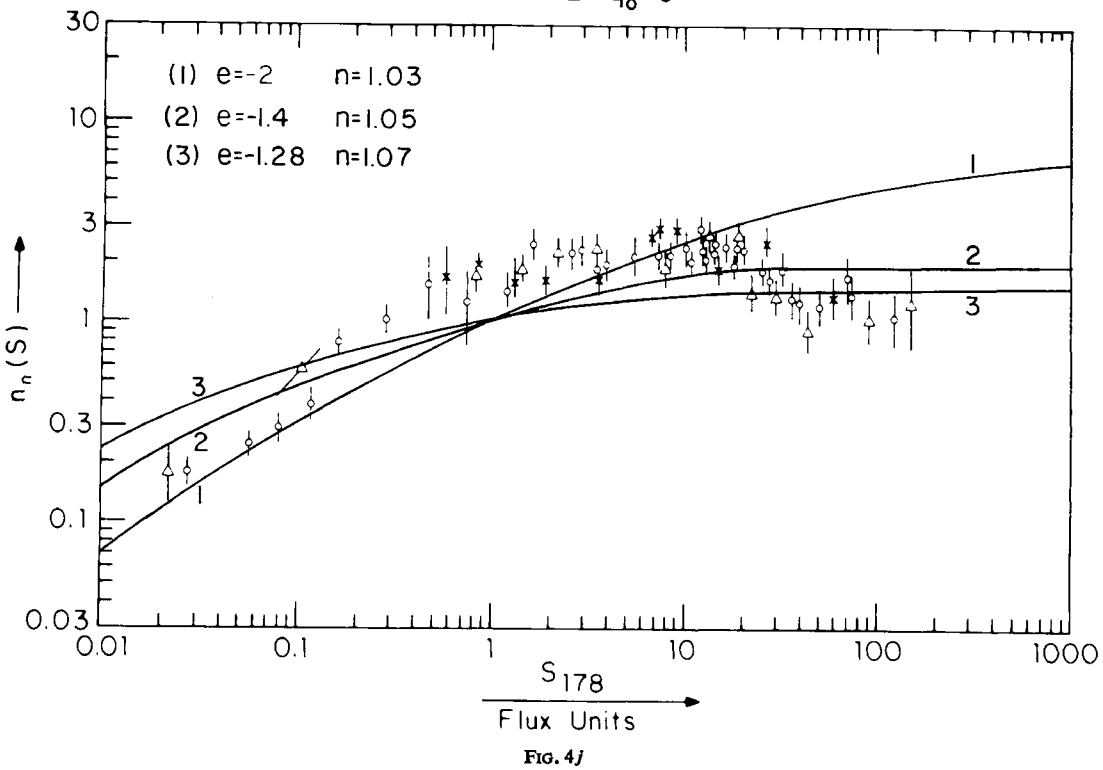


FIG. 4j

Even so, our cosmology brings in an amelioration. In fact, as seen from Table 5, the equivalent $E$ needed here is less than the one usually posited in standard cosmology, as discussed in § I. This means that our differentiation of $\varkappa$ from $z$ has accounted for part of what in standard cosmology is usually lumped under the name "evolutionary corrections." This is not totally unexpected since the luminosity is a function of $G$, which in turn is a function of $t$ and therefore of $z$.

We can conclude by saying that the count of radio sources, much like the optical tests presented in Paper III, not only does not forbid a varying $G$, but can be improved by it.

## REFERENCES


Canuto, V. M., Adams, P. J., Hsieh, S.-H., and Tsiang, E. 1977, *Phys. Rev. D*, **16**, 1643 (Paper I).
Canuto, V. M., and Hsieh, S.-H. 1978, *Ap. J.*, **224**, 302.
———. 1979, *Ap. J. Suppl.*, **41**, 243 (Paper II).
Canuto, V. M., Hsieh, S.-H., and Owen, J. R. 1979, *Ap. J. Suppl.*, **41**, 263 (Paper III).
Dirac, P. A. M. 1938, *Proc. R. Soc. A*, **165**, 199.
———. 1974, *Proc. R. Soc. A*, **338**, 439.
Jauncey, D. L. 1967, *Nature*, **216**, 847.
———. 1975, *Ann. Rev. Astr. Ap.*, **13**, 23.
Petrosian, V. 1969, *Ap. J.*, **155**, 1029.
Rees, M., and Setti, G. 1968, *Nature*, **219**, 127.
Robertson, J. G. 1978, *M.N.R.A.S.*, **182**, 617.
Soltan, A. 1978*a*, *Acta Astr.* **27**, 339.
———. 1978*b*, *Acta Astr.*, **28**, 1.
Véron, P. 1966, *Ann. d'Ap.*, **39**, 231.
von Hoerner, S. 1973, *Ap. J.*, **186**, 741.
Wall, J. V., Pearson, T. J., and Longair, M. S. 1977, in *Proc. IAU Symposium*, **74**, *Radio Astronomy and Cosmology*, ed. D. Jauncey (Dordrecht: Reidel), p. 269.
Weinberg, S. 1972, *Gravitation and Cosmology* (New York: Wiley).


V. M. CANUTO and J. R. OWEN: NASA, Goddard Institute for Space Studies, 2880 Broadway, New York, NY 10025